

The abnormal accumulation of heparan sulfate in patients with mucopolysaccharidosis prevents the elastolytic activity of cathepsin V

Thibault Chazeirat^{a,b}, Sophie Denamur^{a,b,c}, Krzysztof K. Bojarski^d, Pierre-Marie Andrault^e, Damien Sizaret^f, Fuming Zhang^g, Ahlame Saidi^{a,b}, Marine Tardieu^c, Robert J. Linhardt^g, François Labarthe^{c,h}, Dieter Brömme^e, Sergey A. Samsonov^d, Gilles Lalmanach^{a,b}, Fabien Lecaille^{a,b,*}

^a Université de Tours, Tours, France

^b INSERM, UMR 1100, Centre d'Etude des Pathologies Respiratoires (CEPR), Team "Mécanismes Protéolytiques Dans l'Inflammation", Tours, France

^c Pediatric Department, Reference Center for Inborn Errors of Metabolism ToTeM, CHRU Tours, France

^d Faculty of Chemistry, University of Gdańsk, Poland

^e Department of Oral Biological and Medical Sciences, University of British Columbia, Vancouver, British Columbia, Canada

^f Anatomical Pathology and Cytology Department, Bretonneau Hospital, CHRU Tours, France

^g Center for Biotechnology and Interdisciplinary Studies, Rensselaer Polytechnic Institute, Troy, New York, USA

^h INSERM, UMR 1069, Nutrition, Croissance et Cancer (N2C), Tours, France

ARTICLE INFO

Keywords:

Protease
Glycosaminoglycan
MPS
Lung
Elastin

ABSTRACT

Mucopolysaccharidosis (MPS) are rare inherited diseases characterized by accumulation of lysosomal glycosaminoglycans, including heparan sulfate (HS). Patients exhibit progressive multi-visceral dysfunction and shortened lifespan mainly due to a severe cardiac/respiratory decline. Cathepsin V (CatV) is a potent elastolytic protease implicated in extracellular matrix (ECM) remodeling. Whether CatV is inactivated by HS in lungs from MPS patients remained unknown. Herein, CatV colocalized with HS in MPS bronchial epithelial cells. HS level correlated positively with the severity of respiratory symptoms and negatively to the overall endopeptidase activity of cysteine cathepsins. HS bound tightly to CatV and impaired its activity. Withdrawal of HS by glycosidases preserved exogenous CatV activity, while addition of Surfen, a HS antagonist, restored elastolytic CatV-like activity in MPS samples. Our data suggest that the pathophysiological accumulation of HS may be deleterious for CatV-mediated ECM remodeling and for lung tissue homeostasis, thus contributing to respiratory disorders associated to MPS diseases.

1. Introduction

Mucopolysaccharidoses (MPS) are a group of seven rare inherited metabolic diseases associated with deficiencies in enzymes involved in

the degradation of glycosaminoglycans (GAGs). MPS type I (MPS-I) is a lysosomal disease caused by a deficiency of the α -L-iduronidase, which is essential to correct the metabolism of both dermatan sulfate (DS) and heparan sulfate (HS). MPS-I is commonly classified into three clinical

Abbreviations: AEBSEF, 4-(2-aminoethyl) benzenesulfonyl fluoride hydrochloride; CA-074, N-(L-3-trans-propylcarbamoyloxirane-2-carbonyl)-L-isoleucyl-L-proline; Cat, cathepsin; CS, chondroitin sulfate; DMMB, 1,9-dimethylmethylene blue; DS, Dermatan sulfate; DTT, dithiothreitol; E-64, trans-epoxysuccinyl-L-leucylamido(4-guanidino)butane; ECM, extracellular matrix; EDTA, ethylenediaminetetraacetic acid; GAG, glycosaminoglycan; GlcA, glucuronic acid; GlcNAc, N-acetyl-D-glucosamine; GRSS, global respiratory symptoms severity; HA, hyaluronic acid; HS, heparan sulfate; IF, Immunofluorescence; KS, keratan sulfate; MD, molecular dynamics; MMP, matrix metallo-proteinase; MMTS, S-methyl thiomethanesulfonate; MPS, mucopolysaccharidosis; PAS, periodic acid schiff; PMSF, phenylmethylsulfonyl fluoride; ProCat, procathepsin; SPRI, surface plasmon resonance imaging; Surfen, bis-2-methyl-4-amino-quinolyl-6-carbamide hydrate; Z-Phe-Arg-AMC, Z-Phe-Arg-7-amido-4-methylcoumarin.

* Corresponding author at: Université de Tours, INSERM, UMR 1100, CEPR, 10 Boulevard Tonnellé, F-37032 Tours cedex, France.

E-mail addresses: thibault.chazeirat@etu.univ-tours.fr (T. Chazeirat), sophie.denamur@gmail.com (S. Denamur), krzysztof.bojarski@ug.edu.pl (K.K. Bojarski), andrault_pm@yahoo.fr (P.-M. Andrault), D.SIZARET@chu-tours.fr (D. Sizaret), zhangf2@rpi.edu (F. Zhang), ahlame.saidi@univ-tours.fr (A. Saidi), M.TARDIEU@chu-tours.fr (M. Tardieu), linhar@rpi.edu (R.J. Linhardt), francois.labarthe@univ-tours.fr (F. Labarthe), dbromme@dentistry.ubc.ca (D. Brömme), sergey.samsonov@ug.edu.pl (S.A. Samsonov), gilles.lalmanach@univ-tours.fr (G. Lalmanach), fabien.lecaille@univ-tours.fr (F. Lecaille).

<https://doi.org/10.1016/j.carbpol.2020.117261>

Received 27 August 2020; Received in revised form 30 September 2020; Accepted 14 October 2020

Available online 20 October 2020

0144-8617/© 2020 Elsevier Ltd. All rights reserved.

syndromes from severe to attenuated form: Hurler, Hurler-Scheie, and Scheie. MPS-II (or Hunter syndrome) is caused by a deficiency of lysosomal iduronate-2-sulfatase, which is critical for the degradation of both HS and DS, by cleaving their O-linked sulfate. MPS-III (also named Sanfilippo syndrome) is caused by a deficiency in one of the four enzymes involved in the degradation of HS and is divided into four subtypes: heparan N-sulfatase (type IIIA), α -N-acetylglucosaminidase (type IIIB), acetyl CoA: α -glucosaminide acetyltransferase (type IIIC), and N-acetylglucosamine-6-sulfatase (type IIID) (Stapleton et al., 2018). The subsequent accumulation of these GAGs participates in cellular dysfunction, resulting in progressive multi-visceral and tissue damages (Muenzer, 2011). The hallmarks of most MPS-I, II, and III phenotypes are represented by a wide spectrum of clinical severity, including cardiorespiratory diseases, which for the most severe forms of MPS diseases remain the leading cause of early mortality (Arn, Bruce, Wraith, Travers, & Fallet, 2015; Berger et al., 2013; Muhlebach, Wooten, & Muenzer, 2011). Thickened depositions/secretions in airways and interstitium due to an abnormal accumulation of extracellular matrix (ECM) components can further exacerbate obstruction (Batzios, Zafeiriou, & Papakonstantinou, 2013; Leighton, Papsin, Vellodi, Dinwiddie, & Lane, 2001; Pal, Mercer, Jones, Bruce, & Bigger, 2018; Rutten et al., 2016). Under these circumstances, the exact molecular mechanisms by which GAG accumulation ultimately leads to lung disease manifestations have not been clearly elucidated (Iozzo & Gubbiotti, 2018). Therefore, a better understanding of factors affecting airways dysfunction may lead to novel strategies for improving respiratory function in patients with MPS.

Lysosomal cysteine cathepsins are papain-like proteases (eleven members in human: cathepsins B, C, F, H, L, K, O, S, V, X and W) that play key roles in numerous physiological processes in particular the degradation and recycling of endocytosed bulk protein (Lecaille, Kaleta, & Brömme, 2002). Beside their expression in endolysosomal system, cathepsins are also found in cytosol or nucleus and can be secreted (Reiser, Adair, & Reinheckel, 2010; Vidak, Javoršek, Vizovišek, & Turk, 2019). Cathepsins participate in ECM remodeling by degrading major structural proteins (e.g., collagens I, II and IV and elastin), specialized adhesion proteins (e.g., fibronectin, fibrillin, and laminins) and proteoglycan (aggrecan) (Vizovišek, Fonović, & Turk, 2019). Their uncontrolled proteolytic activity (e.g., protease/inhibitor and redox imbalance) is associated with various human diseases including cardiovascular diseases, immune defects, bone and cartilage diseases (osteoporosis, rheumatoid arthritis), cancer, and lung inflammatory pathologies (emphysema, fibrosis, asthma, chronic obstructive pulmonary disease) (for review: Brömme & Wilson, 2011; Lalmanach et al., 2020). Moreover cathepsins are relevant biomarkers and promising therapeutic targets for numerous diseases (Kramer, Turk, & Turk, 2017; Vizovišek et al., 2020). Cathepsins B, C, H, and L are ubiquitously found in mammalian tissues while cathepsins S, K, W, and notably cathepsin V (CatV) exhibit a more restricted expression pattern. CatV (also called CatL2) that shares 80 % protein sequence identity with human CatL is mostly expressed in cornea, testis, epidermis, colon, and thymus (Adachi et al., 1998; Brömme, Li, Barnes, & Mehler, 1999; Santamaría et al., 1998; Tolosa et al., 2003). Deficiency in murine CatL, the orthologue of human CatV, induces myocardial fibrosis probably due to a reduced collagenolytic activity (Spira et al., 2007). A 2-fold reduction of CatV protein level was detected in bronchoalveolar lavage fluids of patients with pulmonary sarcoidosis compared to healthy subjects, suggesting an association to lung matrix homeostasis under physiological and pathological conditions (Naumnik, Ossolińska, Płońska, Chytczewska, & Nikliński, 2014). Human CatV displays a 3-fold higher elastolytic activity than CatK and CatS (Yasuda et al., 2004). In addition, GAGs including chondroitin 4-/6-sulfate (C4-S and C6-S), heparin (Hep) and DS decreased *in vitro* the elastolytic activities of both CatV and CatK and to a lesser extent CatS. Similarly, the digestion of type II collagen by CatK is impaired by the presence of high HS and DS concentrations in osteoclasts from MPS-I mouse model, which likely contributes to MPS-I

bone pathology (Wilson et al., 2009). Previous reports demonstrate that abnormal expression and/or activity of cathepsins B, S, and K correlate with major clinical manifestations in MPS (for review: De Pasquale, Moles, & Pavone, 2020). Nevertheless, it remains unknown whether cysteine cathepsins, and especially elastolytic CatV, contribute to respiratory disorders in MPS.

1.1. Hypotheses

The proteolytic activity of some cysteine cathepsins is tightly controlled by the formation of a complex between their highly positively charged exosites and specific GAGs (for review: Novinec, Lenarčič, & Turk, 2014). Our hypothesis is that *in situ* HS levels in patients with MPS interfere with the proper elastolytic activity of CatV and that this inhibition could be prevented. To address this issue, we evaluated the protein level of CatV and the HS content in respiratory secretions (sputum and tracheal aspirates) of patients with MPS-I, II, and III and unaffected individuals. Also, we characterized CatV elastolytic activity in the presence of HS. Finally, we demonstrated that Surfen, a small HS antagonist, markedly restored the endogenous elastolytic CatV-like activity in MPS samples.

2. Material and methods

2.1. Reagents

Benzoyloxycarbonyl-Phe-Arg-7-amino-4-methyl coumarin (Z-Phe-Arg-AMC) was purchased from R&D Systems (R&D Systems Europe, Abingdon, UK). E-64 (1-3-carboxy-trans-2-3-epoxypropionyl-leucylamido-(4-guanidino)-butane), Pepstatin A, EDTA, 4-(2-aminoethyl) benzenesulfonyl fluoride hydrochloride (AEBSF, Pefabloc), S-methyl thiomethanesulfonate (MMTS) and Elastin-Congo Red conjugate were obtained from Sigma-Aldrich (Saint Quentin Fallavier, France). CatB inhibitor N-(L-3-trans-propylcarbamoyloxirane-2-carbonyl)-L-isoleucyl-L-proline (CA-074) and CatL inhibitor (N-(4-biphenylacetyl)-S-methylcysteine-(D)-Arg-Phe- β -phenethylamide, a.k.a CatL inh. 7) (Chowdhury et al., 2002) were from Calbiochem (Merck Millipore, France). CatS inhibitor (morpholinourea-leucyl-L-homophenylalanine-vinyl-sulfone phenyl inhibitor, LHVS) was a kind gift from Dr. J. H. McKerrow (Skaggs School of Pharmacy and Pharmaceutical Sciences, University of California, San Diego, USA). Odanacatib (CatK inhibitor) was from Selleck Chemicals (Houston, TX, U.S.A.). Heparan sulfate (HS) from bovine kidney (~14 kDa), chondroitin 4-sulfate (C4-S) from bovine trachea (20–30 kDa), chondroitin 6-sulfate (C6-S) from shark cartilage (~63 kDa), dermatan sulfate (DS) from porcine intestinal mucosa (~14 kDa), dermatan sulfate (DS) from porcine intestinal mucosa (~14 kDa), heparin (Hep) from porcine intestinal mucosa (15–17 kDa), hyaluronic acid (HA) from *Streptococcus equi* (~1400 kDa) were from commercial source (Sigma-Aldrich). Perlecan isolated from basement membrane extract (derived from Engelbreth-Holm-Swarm mouse sarcoma) and aggrecan from bovine articular cartilage were supplied by Sigma-Aldrich. Insoluble elastin from bovine neck was a kind gift from Dr. Laurent Duca (UMR CNRS 7369 MEDyC, Reims, France). Surfen (bis-2-methyl-4-amino-quinolyl-6-carbamide hydrate) came from Sigma-Aldrich.

2.2. Enzymes

Heparinases I, II, III, Δ -4,5-glycuronidase, and chondroitinase B, all from *Flavobacterium heparinum* were purchased from Grampenz (Upper Ardoe, Aberdeen, Scotland). Dnase I from bovine pancreas was purchased from Sigma-Aldrich. Recombinant human procathepsin V (pro-CatV) was cloned in the pPic9K yeast expression system and expressed in *Pichia pastoris* as previously described (Brömme et al., 1999). The K20 G CatV mutant was generated with the following primers, forward: 5'-AAGAATCAGGGACAGTGTGGTTCTTGTT-3', and reverse:

5'-CACTGGCGTCACGTAGCCTT-3', using the pPic9K vector carrying the wild-type proCatV sequence as a template. The expression of the recombinant wild-type (wt) CatV and K20 G CatV mutant, extraction, as well as renaturation, purification and processing into active form were carried out as previously described (Du, Chen, Wong, Craik, & Brömme, 2013). Unless stated otherwise, enzymatic assays for cathepsin activity were carried out in 100 mM sodium acetate buffer, pH 5.5 containing 2 mM dithiothreitol (DTT). Cathepsin activity was recorded using as substrate Z-Phe-Arg-AMC ($\lambda_{\text{ex}} = 350 \text{ nm}$, $\lambda_{\text{em}} = 460 \text{ nm}$, Spectramax Gemini spectrofluorometer, Molecular Devices, Saint Grégoire, France). The active site concentrations of wild-type CatV and K20 G CatV mutant were determined using E-64 (Barrett et al., 1982).

2.3. MPS-I lung biopsy

Postmortem lung tissue samples from a 2-year old female with MPS type I were kindly provided by Dr Michael McDermott (Department of Histopathology, Dublin, Ireland). Autopsy findings suggested a cardiopulmonary pathology in combination with transplant related pulmonary venopathy (Gupta, O'Meara, Wynn, & McDermott, 2013). Samples were further used for staining, immunohistological (IHC) and immunofluorescence (IF) examinations.

2.4. Lung biological samples from MPS and non-MPS patients

Sputum and tracheal aspirates (respiratory specimens) from MPS patients (N = 11, including 2 MPS-I, 5 MPS-II, and 4 MPS-III) and non-MPS patients (controls, N = 9) were collected in the Pediatric and Intensive Care Units of the University Hospital of Tours, France. Respiratory-related disorders were evaluated by three independent clinicians for MPS patients as part of routine follow-up. Based on the analysis criteria from early comprehensive literature surveys (Berger et al., 2013; Muhlebach et al., 2011), a global respiratory symptoms severity (GRSS) evaluation was assessed for each patients regarding four sub-types: ear-nose-throat symptoms (chronic rhinitis or sinusitis, otitis, adeno-tonsillar hypertrophy, hearing loss, macroglossia, stridor), pulmonary symptoms (dyspnea, wheezing, cough, sputum, asthma, bronchitis, pneumonia), clinical symptoms of obstructive sleep apnea, and skeletal abnormalities causing restrictive lung disease (scoliosis, kyphosis, ribcage narrowing, chest wall deformity). The GRSS was graduated from 0 to 4, corresponding to the number of respiratory disorder sub-types reported for each patient. This study was approved by the French National bioethical authorities (n°ID-RCB: 2019-A01361-56) and informed written consent was obtained from parents of each participant. Non-MPS patients were intubated for cardiac surgery or severe head trauma. None of the patients in the control group had chronic respiratory disease before admission or breathing symptoms during hospital stay. Tracheal aspirations of MPS and control groups were taken during an orotracheal intubation of the patient in the operating room or in the Pediatric Intensive Care Unit (University Hospital of Tours, France). Samples were aseptically weighed, instantly diluted at 1 g/10 mL in a preservative buffer (100 mM sodium acetate, pH 5.0 plus the peptidase inhibitors 0.5 mM PMSF, 0.5 mM EDTA, 40 μM pepstatin A, and 1 mM MMTS) (Naudin et al., 2011), then centrifuged for 10 min at 5000 g at 4 °C. Resulting cell-free supernatants were collected, aliquoted and stored at -80 °C. The total protein quantification of supernatants was performed by BCA assay (ThermoFisher Scientific).

2.5. Immunohistological and immunofluorescence studies in MPS-I lung tissue sections

Samples were fixed in neutral-buffered, 10 % formalin solution and processed by standard methods for further histological examinations. Conventional immunohistochemistry was performed on automatic BenchMark XT (Roche). The lung parenchyma was stained with

Hematoxylin-Eosin-Safran (HES) (Tissue-Tek Prisma, Sakura Finetek Europe). Periodic Acid Schiff (PAS) was used to detect polysaccharides. In parallel, anti-CD68 (a monocyte and macrophage marker, 1:200, Dako) was used as control. Finally, digital microscopic images were acquired from scanned slides (Hamamatsu Nanozoomer 2.0RS, magnification: x200 to x400) and processed with the Hamamatsu NDP.view 2.0 software. The immunohistochemical detections of CatV and HS were obtained without antigen retrieval after removing paraffin with xylene. Tissue sections were rehydrated by sequential washings with ethanol and water. Briefly, the endogenous peroxidase activity was blocked by incubating sections in 3% H₂O₂ solution for 20 min. Non-specific binding sites were blocked with 5% BSA in PBS for 1 h at room temperature. Sections were then incubated overnight at 4 °C with goat anti cathepsin V (1:400 dilution in PBS with 5% BSA, R&D Systems), and mouse anti heparan sulfate (10E4: 1:400 dilution in PBS with 5% BSA, Amsbio, Cambridge, MA, USA). The slides were washed and further incubated with peroxidase-conjugated goat anti-mouse or mouse anti-goat IgG (1:1,000, R&D Systems) for 1 h. Peroxidase activity in tissue sections was visualized as brown color using 3, 3'-diaminobenzidine as a substrate solution. Lung sections were counterstained with Gill's hematoxylin for 1 min, dehydrated, cleared in xylene, and mounted in Vectamount permanent medium (Vector Labs, Peterborough, U.K.)

2.5.1. Immunofluorescence (IF) assays on CatV and HS

Non-specific binding sites were blocked with PBS containing 5% BSA and 5% goat serum for 2 h, at room temperature. Sections were then incubated overnight at 4 °C with goat anti-CatV (1:100 dilution in PBS containing 5% BSA and 5% goat serum) and mouse anti-HS 10E4 (1:100 dilution in PBS containing 5% BSA and 5% goat serum). Slides were washed and further incubated with fluorescein-labeled anti-mouse IgM antibody (1:2,000, Molecular Probes) or anti-goat IgG NorthernLights™ NL637-conjugated antibody (1:2,000, R&D Systems) for 1 h. Lung sections were counterstained with DAPI (4',6-diamidino-2-phenylindole) for 1 min, and mounted in Vectamount permanent medium (Vector Labs., Peterborough, U.K.). Microscopic images were acquired (Carl Zeiss Axio vert A1 inverted microscope, magnification: x200) and processed with the ZEISS microscope software, ZEN 2 Lite blue and repeated three times on three separate tissue sections. The lack of cross reactivity of anti-CatV antibody was checked by western blot analysis on human cathepsins B, K, L, and S (100 ng) as described elsewhere (Sage et al., 2013).

2.6. Cathepsin V and sulfated GAGs in MPS biological samples

Following running of MPS cell-free supernatants (50 μg of total protein/well; 12 % SDS-PAGE under reducing conditions) CatV was immunodetected by a mouse anti CatV primary antibody (1:1,000) incubated overnight at 4 °C. Horseradish peroxidase (HRP)-conjugated anti-IgG antibody (1:5,000) was incubated for 1 h at room temperature, and immune-positive bands were visualized using an enhanced chemiluminescence assay kit (ECL Plus Western blotting detection system; Amersham Biosciences, UK). Assays (triplicate) were repeated at least three independent times. In addition, a quantitative analysis of CatV was performed in MPS and non-MPS cell-free supernatants using a sandwich ELISA DuoSet kit (R&D Systems).

Sulfated GAGs were quantified with 1,9-dimethylmethylene blue (DMMB, Sigma-Aldrich), (Barbosa et al., 2003). Absorbance was measured at 654 nm (Cary 100 spectrophotometer, Agilent, France) and all values were reported to a final protein content (100 μg). Finally, concentrations of sulfated GAGs were determined by using a calibration curve of similarly treated commercial C4-S solutions (1–10 $\mu\text{g}/\text{mL}$). In parallel, CS, DS and HS content in MPS and non-MPS biological samples were determined by ELISA (AMS Biotechnology, Abingdon, UK) (n = 3, triplicate).

2.7. Titration of cathepsins in MPS and non-MPS lung biological samples

Overall endopeptidase cysteine cathepsin concentration in cell-free supernatants (sputum and tracheal aspirates: 30 µg of total protein) from MPS and non-MPS patients, as reported elsewhere (Naudin et al., 2011). Assays were performed in triplicates and repeated at least three times.

2.8. Activity of exogenous cathepsin V in the presence of biological samples

The activity of recombinant CatV (0.5 nM) was measured *in vitro* at 37 °C without or with increasing amounts of cell-free supernatants (corresponding to 3–300 ng of total protein) from sputum and tracheal aspirates of MPS patients in 100 mM sodium acetate buffer, pH 5.5, 0.01 % Brij35, 10 mM DTT, using Z-Phe-Arg-AMC (20 µM) as a substrate. The activity was measured by spectrofluorometry ($\lambda_{\text{ex}} = 350$ nm, $\lambda_{\text{em}} = 460$ nm). The same experiment was carried out with biological samples pretreated with glycosidases (heparinase I, II, and III, chondroitinase B, and Δ -4,5-glycuronidase) (180 mU/mL), sodium chromate (10 mM), and Dnase I (100 mU/mL) during 48 h at 37 °C under vigorous agitation. Controls were performed with non-MPS patients. All kinetic measurements were made in triplicates and repeated three times independently.

2.9. Activity of recombinant cathepsin V in the presence of CHO cell-free lysates

Chinese Hamster Ovary (CHO) cell lines K1 (HS positive, American Type Culture Collection: ATCC, code CCL-61) and 2244 (HS negative, pgsD-677, ATCC code CRL-2244) were a kind gift from Dr. Romain Vivès (Institut de Biologie Structurale, Grenoble, France). CHO cells were cultured at 37 °C, under 5% CO₂, in EMEM supplemented with 10 % fetal calf serum, penicillin (50 IU/mL), and streptomycin (50 µg/mL). CHO cells were harvested at a density of approximately 2×10^6 cells/mL, centrifuged at 200 g for 10 min, then washed once with the preservative buffer (100 mM sodium acetate, pH 5.0, 0.5 mM PMSF, 0.5 mM EDTA, 40 µM pepstatin A, and 1 mM MMTS). The cell pellet was resuspended to achieve a density of approximately 5×10^8 cells/mL. Cell lines K1 and 2244 disruption was accomplished by syringing the harvested cell pellet through a 20-gauge needle, and CHO cell-free supernatants were recovered after centrifugation (10,000 g, 10 min). Protein concentration was determined by a BCA assay, while sulfated GAGs and HS contents were measured using DMMB and ELISA assays, respectively. CatV (1 nM) was incubated with each cell lysate (K1 and 2244, 50 µg of total protein) in 100 mM sodium acetate buffer pH 5.5 containing 2 mM DTT. The residual activity was measured after addition of Z-Phe-Arg-AMC (20 µM) ($\lambda_{\text{ex}} = 350$ nm, $\lambda_{\text{em}} = 460$ nm). Assays were repeated under the same conditions using CHO K1 cell-free supernatants pretreated with a solution containing glycosidases (heparinase I, II, and III, chondroitinase B, and Δ -4,5-glycuronidase) (180 mU/mL), sodium chromate (10 mM), and Dnase I (100 mU/mL) for 48 h at 37 °C under robust agitation. All kinetic measurements were performed in triplicates and repeated three times.

2.10. Complex formation between cathepsin V and HS

Recombinant CatV (1 µg) was incubated in the presence or absence of HS (0.15 %, w/v, 14 kDa) in a final volume (100 µL) for 10 min in 100 mM sodium acetate buffer, pH 5.5. Samples were then applied to a size exclusion Superdex 200 column (AKTA purifier 900 HPLC system, Amersham, GEHealthcare Bio-Sciences AB, Uppsala, Sweden), previously equilibrated in the same buffer. Protein elution was monitored at 280 nm. The calibration curve was obtained using the standard protein molecular mass markers (Amersham). CatV enzymatic activity was recorded for each fraction (0.5 mL) using Z-Phe-Arg-AMC (20 µM) as substrate. Immunoreactive CatV was detected using a polyclonal goat

anti-human CatV antibody (1:1,000) as described previously. HS was revealed in collected fractions using the DMMB assay. Alternatively, dissociation equilibrium constant (K_D) determination between recombinant CatV and HS (0.15 %) was measured by surface plasmon resonance imaging (SPRI), as reported elsewhere (Sage et al., 2013).

2.11. Molecular modeling of interactions between cathepsin V and HS

Autodock 3 was first used for docking HS, heparin and C4-S tetrasaccharide to CatV (PDB ID: 1 FH0) (Morris et al., 1998). The ligands were modeled using GLYCAM06 parameters (Kirschner et al., 2008). The charges of the ligands were previously integrated into the corresponding libraries of GAG monomeric units (Pichert et al., 2012). The protocols for molecular docking and clustering previously optimized for protein-GAG systems were used (Panitz et al., 2016). Structures of CatV/GAG complexes were then used for molecular dynamics (MD) simulations with AMBER 14 (Case, Cerutti, Cheatham, Darden, & Duke, 2017). The details for the MD protocols are detailed elsewhere (Panitz et al., 2016). Free energy calculations and per residue decomposition were performed using Molecular Mechanics-Generalized Born Surface Area (MM-GBSA) with $gb = 2$ (Onufriev, Case, & Bashford, 2002) implemented in AMBER for 100 frames evenly distributed in the productive MD run. Analysis of the trajectories was done using the cpptraj module of AMBER and VMD for visualization (Humphrey, Dalke, & Schulten, 1996). Alternatively, assays were performed on CatL (PDB ID: 2XU3).

2.12. Kinetic parameters of wild-type cathepsin V and K20 G cathepsin V mutant with GAGs

CatV (0.5 nM) was incubated 10 min in the activity buffer in the presence or absence of HS, C4-S, C6-S, Hep, DS, and HA, respectively (0.15 and 0.3 %, w/v) at 37 °C. CatV activity was then monitored using Z-Phe-Arg-AMC (20 µM) as a substrate. Experiments with HS were repeated in the presence of increasing amount of NaCl (0–0.5 M). Assays (triplicate) were achieved three times in separate experiments, and relative data are given as means \pm SD. Steady-state kinetics were assessed as previously described (Sage et al., 2013). Similar assays were repeated with K20 G CatV (0.5 nM) and HS (0.15 %, w/v).

Further, the peptidase activity of CatV was recorded in the presence of increasing amounts of HS (0–0.01 %), using Z-Phe-Arg-AMC (1–20 µM) as substrate. Data were plotted using the equation $1/V = f(1/S)$ (*i.e.*, Lineweaver-Burk plot). Inhibition data were fit by nonlinear regression analysis using the non-competitive model inhibition to determine the equilibrium dissociation constant (K_i) (GraphPad Software). All measurements were performed three times in triplicate.

2.13. Inhibition of cathepsin V by perlecan and HS derivatives

CatV (0.5 nM) activity was measured in the presence or absence of perlecan (0.1–2 µg/mL), aggrecan (0.1–2 µg/mL), and synthetic HS di-(dp2) and tetra-saccharide (dp4; 0.001–0.005%, w/v) (Liu et al., 2010) in the activity buffer, using Z-Phe-Arg-AMC (20 µM) as a substrate. Control experiment was carried out with perlecan (2 µg/mL) pretreated with heparinase I (2 U/mL) in the activity buffer during 15 min at 37 °C. Assays were repeated in the presence of Surfen (10 µM). All measurements were performed three times in triplicate.

2.14. Inhibition of the elastolytic activity of cathepsin V by HS

Elastin-Congo Red conjugate (10 mg/mL) was incubated at 37 °C overnight under vigorous agitation with MPS samples (50 µg of total protein) in 100 mM sodium acetate buffer, pH 5.5 containing 10 mM DTT, in the presence or absence of Surfen (10 µM). Controls were performed by preincubating previous mixtures with cathepsin inhibitors: E-64 (100 µM), CA-074 (1 µM), CatL inh.7 (1 µM), LHSV (10 nM) and

Odanacatib (1 μM). In another set of experiments, aliquots of 10 mg/mL of elastin-Congo Red conjugate were incubated with wild-type CatV (1 μM) or K20 G CatV (1 μM) in the presence or absence of HS (0.15 %) in 100 mM sodium acetate buffer, pH 5.5 containing 2 mM DTT, and the mixture was vigorously vortexed at 37 °C overnight. All assays were stopped by centrifugation (13,500 g, 4 °C) to remove the supernatant from the insoluble contents (pellet). The absorbance of the supernatant was measured at 490 nm by spectrophotometry (Cary 100 spectrophotometer, Agilent). All measurements were performed three independent times in triplicate. Similar experiments were repeated under the same conditions with insoluble elastin from bovine neck (10 mg/mL) in the absence and presence of CatV (1 μM) for scanning electron microscopy. Pellets were then fixed by incubation for 24 h in 4% paraformaldehyde, 1% glutaraldehyde in 0.1 M phosphate buffer (pH 7.2). Afterwards, samples were then washed in phosphate-buffered saline (PBS), post-fixed by incubation with 2% osmium tetroxide for 1 h, then dehydrated by ethanol and dried in hexamethyldisilazane (HMDS, Sigma-Aldrich). Finally, samples were coated with 40 Å platinum, using a GATAN PECS 682 apparatus (Pleasanton, CA, USA), before observation under a Zeiss Ultra plus FEG-SEM scanning electron microscope (Oberkochen, Germany).

2.15. Statistical analysis

Data were expressed as mean \pm SD unless indicated. Statistical significance between the different values was analyzed by non-parametric Mann-Whitney *U* test and patients groups comparison were performed with non-parametric Wilcoxon test. Statistical analysis was performed using GraphPad Prism (GraphPad software, San Diego, CA, USA). Differences at a *P*-value < 0.05 were considered significant.

3. Results

3.1. Cathepsin V and heparan sulfate colocalize in MPS-I lung biopsy

The expression of CatV in lung tissue from a 2-year old female with MPS-I (Hurler syndrome) was investigated by IHC (Fig. 1). Main clinical and pathological details have been described previously (Gupta et al., 2013). Briefly, the stained lung tissue sections showed pulmonary parenchyma and bronchial structures modified by autolysis lesions due to the autopsy delay. Malformation or dystrophic arteriolar vascular lesions were observed with edematous and concentric wall fibrosis (Fig. 1A), harboring well-formed granulomas with resorptive multinucleated giant cells (MNGCs) containing few lipid crystals deposits (Fig. 1B). Well-formed granulomas were less present in the alveolar walls. Numerous plump alveolar macrophages with vacuolated cytoplasm were identified in alveolar spaces (Fig. 1C), including cases engorged with Periodic Acid Schiff positive material (Fig. 1D, e.g., glycoprotein, carbohydrate and mucins-like structures). Cells, especially endothelial and bronchial epithelial cells, ubiquitously expressed significant amount of CatV (Fig. 1E, F). Moreover, a fluorescence overlay of CatV and HS probes was observed predominantly in bronchial epithelial cells in MPS-I lung tissue, suggesting a possible co-localization (Fig. 1G).

3.2. Cathepsin V and heparan sulfate levels in MPS-I, II, and III respiratory samples

Given the scarcity of lung biopsies from young MPS patients, we decided to use as biological specimen sputum and tracheal aspirates. Eleven MPS patients with a history of respiratory complaints, and nine non-MPS patients with no respiratory symptoms were recruited. MPS patient characteristics were summarized in Table 1. There were more males, which reflects the disease population (in particular MPS-II, an X-linked disease affecting mainly males). The mean age, size and weight of the MPS patients (10 \pm 6 years; 112.3 \pm 18 cm; 26.5 \pm 11 kg) were not statistically different than control groups (9 \pm 6 years; 133 \pm 41; 34 \pm

22 kg).

The global respiratory symptoms severity (GRSS) score was assessed for each patient on the basis of four sub-type evaluations: ear-nose-throat symptoms (chronic rhinitis or sinusitis, otitis, adeno-tonsillar hypertrophy, hearing loss, macroglossia, stridor), pulmonary symptoms (dyspnea, wheezing, cough, sputum, asthma, bronchitis, pneumonia), clinical symptoms of obstructive sleep apnea, and skeletal abnormalities causing restrictive lung disease (scoliosis, kyphosis, rib-cage narrowing, chest wall deformity). The GRSS was graduated from 0 to 4, corresponding to the number of sub-types symptoms reported for each patient.

The expression levels of CatV in cell-free supernatants of induced sputum and tracheal aspirates of MPS patients was evaluated by Western-blot and ELISA (Fig. 2). Both pro-CatV (as full or partially processed proforms) and mature CatV were detected by Western blots analysis (Fig. 2A). We did not find a significant difference in expression level of immunoreactive CatV (ELISA assay) between MPS patients and non-MPS patients (379 \pm 181 pg/mL vs. 439 \pm 256 pg/mL, normalized to total homogenate protein content of 100 μg in each sample) (Fig. 2B). Also, there was no difference in CatV levels between MPS types (supplementary Fig. 1A). Conversely, ELISA analysis demonstrated that all MPS patients displayed a 4-fold increase of HS levels (19.3 \pm 10 ng/mL) compared to controls (3.9 \pm 4 ng/mL) (*P* < 0.0001) (Fig. 2C). Nevertheless, no significant difference of HS levels was observed between MPS types (supplementary Fig. 1B). DS levels were lower (5 \pm 8 ng/mL) than HS in MPS patients, but higher compared to controls (1 \pm 1 ng/mL) (*P* < 0.05, Fig. 2D). No significant difference was observed for chondroitin sulfate (CS) between MPS and non-MPS patients (supplementary Fig. 1C). Present data suggest that, among major lung sulfated GAGs, HS concentration is increased substantially in respiratory samples from MPS types I, II, and III. Of note, a significant increase of total sulfated GAGs content (DMMB test) was measured in MPS patients vs. controls (*P* < 0.0001) (supplementary Fig. 1D). Nevertheless, the total sulfated GAGs levels ($\mu\text{g}/\text{mL}$) was higher than HS, DS, and CS levels (pg/mL), this difference probably depending on the presence of other sulfated GAGs, proteoglycans or DNA fragments, which may interact with DMMB as reported by Barbosa et al. (Barbosa et al., 2003). We expanded our observations by comparing HS levels in respiratory samples from the cohort of MPS patients on the basis of the global respiratory symptoms severity (GRSS) (Fig. 2E). Interestingly, the GRSS scores correlated positively ($r_s = 0.91$, *P* < 0.0001) with HS concentration, suggesting that an elevated HS level is associated with the onset of respiratory-related disorders. In addition, the GRSS scores correlated positively with the age of MPS patients ($r_s = 0.6515$, *P* < 0.0354, supplementary Fig. 1E), supporting that accumulation of GAGs leads to diverse clinical manifestations including respiratory problems that worsen with age.

3.3. Cathepsin V activity in MPS-I, II, and III samples

A former report showed that elevated HS concentrations impair CatV activity *in vitro* (Yasuda et al., 2004). Accordingly, we evaluated the ability of HS-enriched MPS samples to inhibit CatV (Fig. 3). We first measured the total endopeptidase activity of cysteine cathepsins in cell-free supernatant from both MPS and non-MPS samples, using Z-Phe-Arg-AMC as a broad-spectrum substrate, and E-64 as titration reagent. A \sim 2.5-fold decrease of active cathepsins was measured in all MPS types (259 \pm 74 nM) compared with controls (616 \pm 296 nM) (Fig. 3A; *P* < 0.05). Also, this drop of active forms of cathepsins correlated negatively (Fig. 3B; $r_s = -0.66$; *P* = 0.0015) with HS levels and sulfated GAG content ($r_s = -0.79$; *P* < 0.0001, supplementary Fig. 1F), and with the GRSS scores (Fig. 3C; $r_s = -0.7052$; *P* = 0.0005). Due to a lack of both selective substrate and inhibitor of CatV, an indirect method was devised to uncover the influence of GAG on CatV activity. Three serial dilutions of cell-free supernatants (corresponding to 300, 30, and 3 ng of total protein, respectively) were mixed with a constant amount of exogenous recombinant CatV (0.5 nM), before monitoring the residual

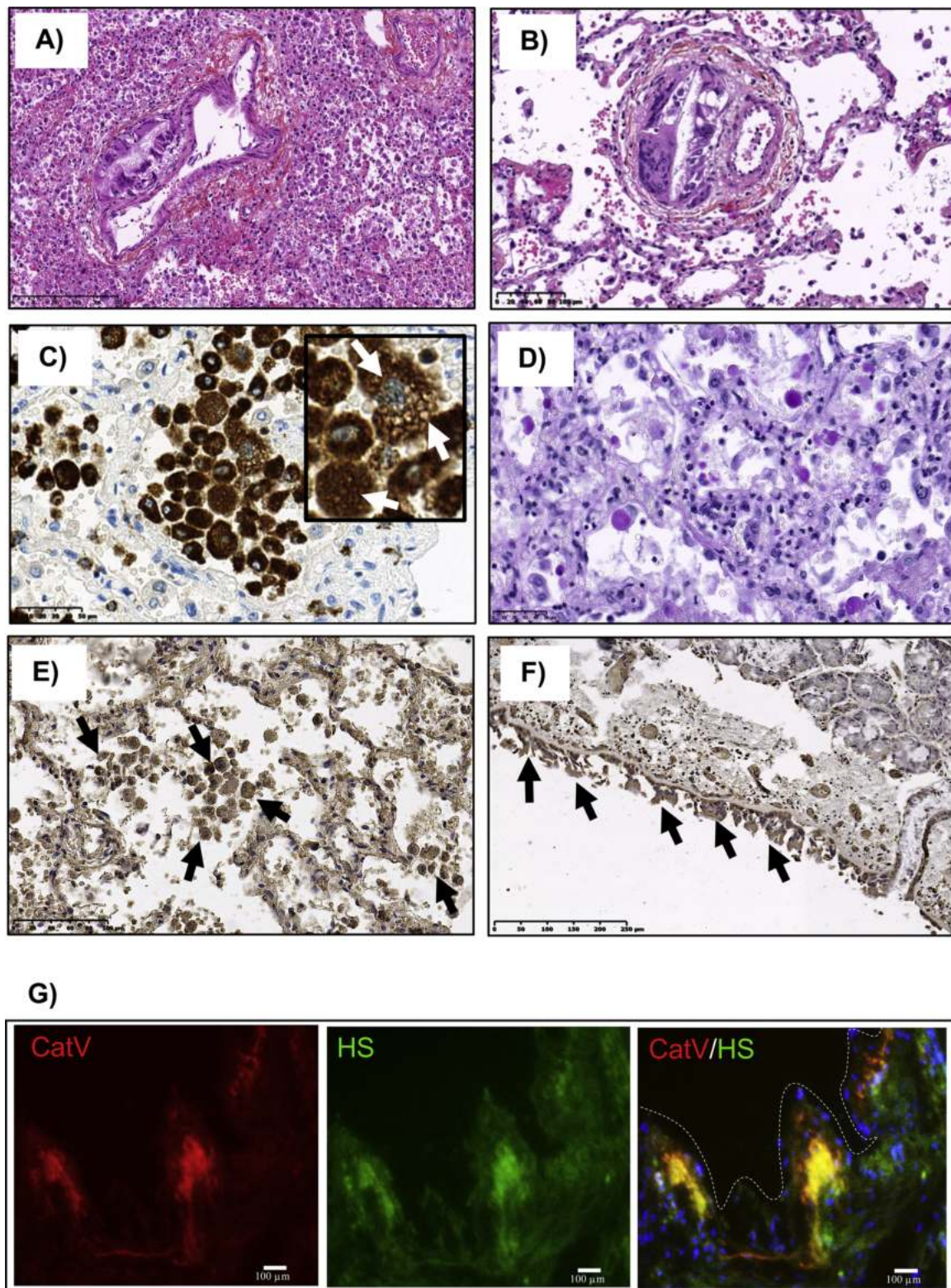


Fig. 1. Immunodetection of cathepsin V in MPS-I lung tissue. Hematoxylin eosin saffron (HES) staining (panels A and B), CD68 IHC (panel C), PAS staining (panel D), CatV IHC (panels E and F), and CatV/HS IF (panel G) were performed on lung tissue obtained from a post-mortem 2-year-old female with MPS-I. A) Mild concentric edematous fibrosis of blood vessels (x10). B) Granuloma exhibiting multinucleated giant cells in venular walls (x20). C) Alveolar macrophages with numerous vacuoles (white arrows) in the cytoplasm (inset) (x40). D) Eosinophils and mucopolysaccharides deposits mainly in alveolar macrophages (x40). E) CatV in alveolar macrophages (x300) and F) in bronchial cells (x150), as indicated by black arrows. G) Representative IF images (of two independent experiments performed) showing CatV stained in red and HS in green. Merged panel revealed the co-localization of both antigens in bronchial cells. Cell nuclei were stained in blue (DAPI staining). Scale bar is 50 μm (panels C, D), 100 μm (panels B, E, G), and 250 μm (panels A, F).

Table 1
Clinical characteristics of MPS patients.

#	Age (yr)	Sex	Weight (kg)	Height (cm)	Diagnosis (MPS type, subtype)	Enzyme deficiency	Treat-ment	GRSS score
1	11	M	22.3	104	Hurler (I)	IDUA	ERT	4
2	14	F	24.8	106	Hurler (I)	"	ERT	4
3	2	M	14.4	85	Hunter (II)	IDS	ERT	2
4	8	M	49.5	125	Hunter (II)	"	ERT	3
5	4	M	20.5	105	Hunter (II)	"	ERT	2
6	2	M	14.1	90	Hunter (II)	"	ERT	2
7	19	M	22.9	114	Hunter (II)	"	ERT	4
8	7	M	29.4	118	San Filippo (III, A)	HNS	no	3
9	18	F	33.4	127	San Filippo (III, B)	NAG	no	2
10	15	M	40.0	149	San Filippo (III, B)	"	no	4
11	6	M	20.8	112	San Filippo (III, C)	HGSNAT	no	1

IDUA: α -L-iduronidase; IDS: iduronate-2-sulfatase; HNS: heparan-N-sulfatase; NAG: N-acetyl-glucosaminidase; HGSNAT: heparan α -glucosaminide-N-acetyltransferase; ERT: enzyme replacement therapy; no: no specific treatment. MPS patients were assigned with a number (#).

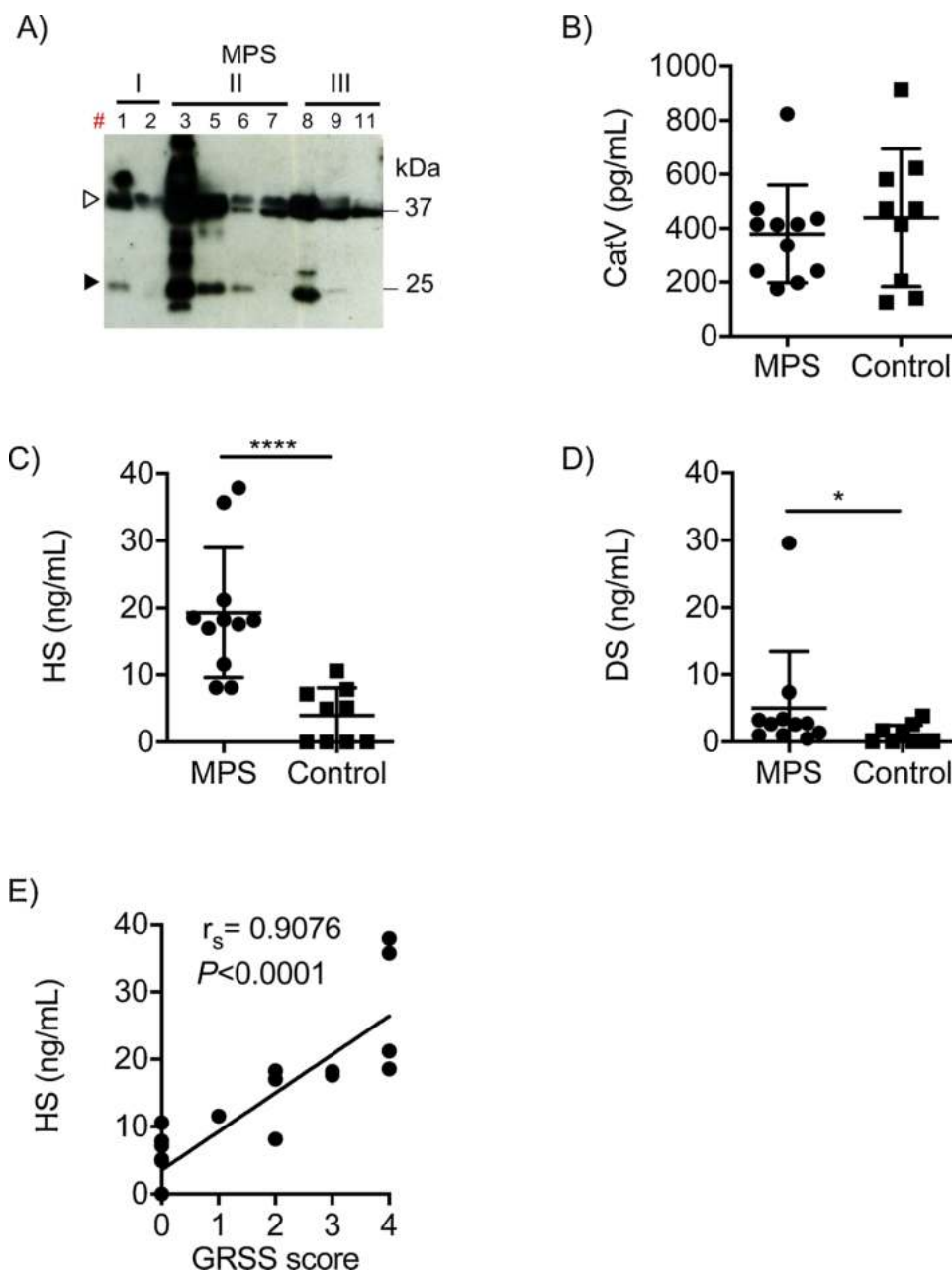


Fig. 2. Cathepsin V and heparan sulfate levels in respiratory secretions from MPS-I, II, and III patients.

A) Representative western blot (of two independent experiments) reflecting CatV protein expression (white and black arrows: pro- and mature form, respectively) in cell-free supernatants from MPS-I, II, and III respiratory secretions (total protein deposited: 50 μ g/well). Number (#) assigned to each MPS patient refers to Table 1. Two MPS (type II and III B) samples were not shown due to their limited availability for western blot. B) ELISA protein levels of CatV in MPS (N = 11) and non-MPS patients (control, N = 9). C) HS concentration determined by ELISA. D) DS concentration determined by ELISA. E) Correlation between HS levels and global respiratory symptoms severity (GRSS) score. The GRSS score was graduated from 0 to 4, corresponding to the number of major clinical respiratory signs/symptoms diagnosed for each patient. Study was completed by linear regression. Spearman coefficient (r_s) and level of significance (P) were reported. Statistical analyses were performed using Mann-Whitney U test, (**: $P < 0.01$; ****: $P < 0.0001$). Results are expressed as mean \pm standard deviation (SD) of three independent experiments.

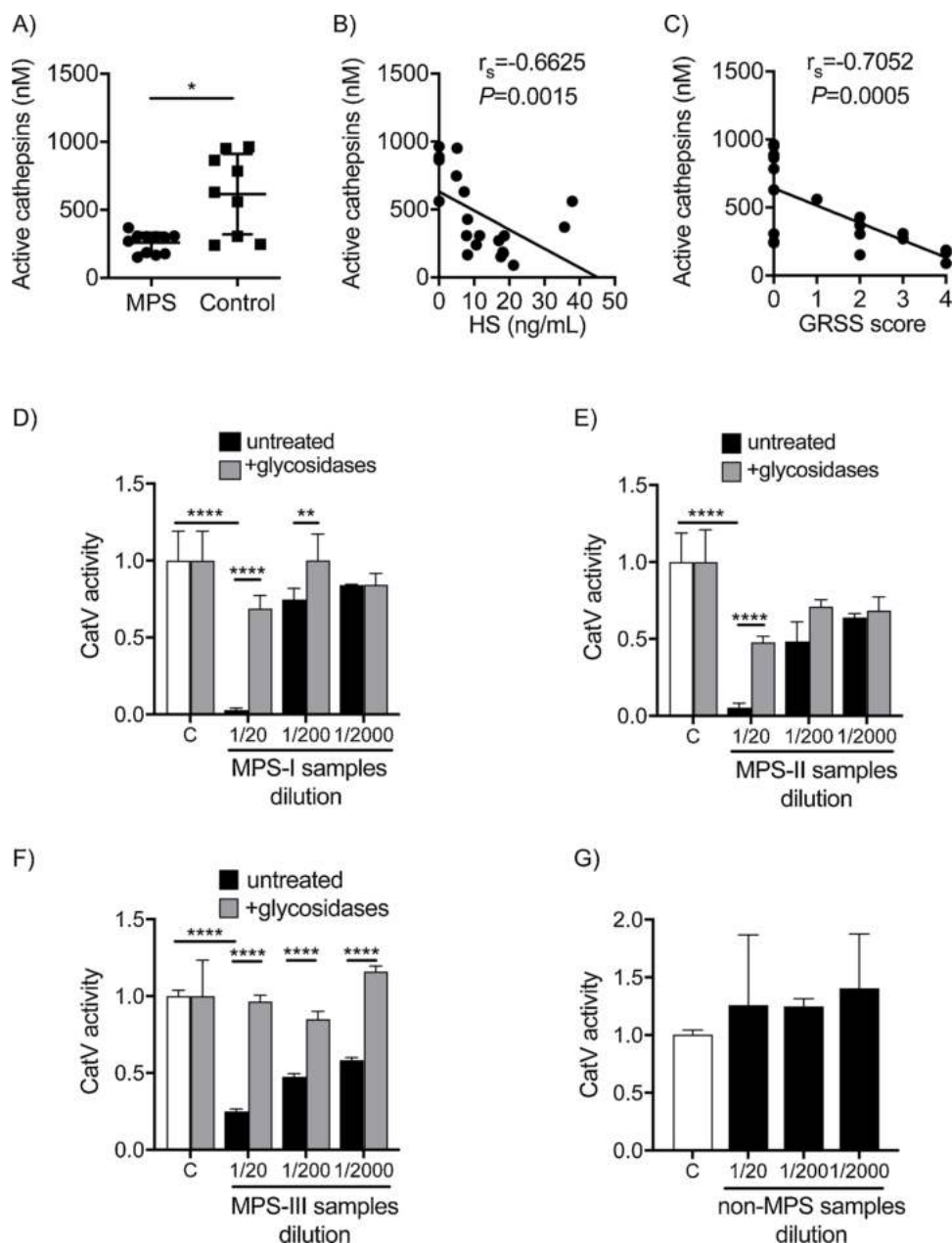


Fig. 3. Inhibition of cathepsin V in respiratory secretions from MPS-I, II, and III patients.

A) Active cathepsins concentration was determined by E-64 titration (MPS and non-MPS samples; 30 μ g of total protein). B) Correlation between concentrations of active cysteine cathepsins and HS level. C) Correlation between concentrations of active cysteine cathepsins and GRSS score. D) Recombinant CatV (0.5 nM) was incubated for 10 min in the activity buffer alone (control: C) or with different dilutions of cell-free supernatants from individual respiratory secretion of MPS-I (N = 2), E) MPS-II (N = 5), F) MPS-III (N = 4), and G) non-MPS (N = 9). The same experiment was carried out with samples pre-treated with glycosidases (heparinases I, II, III, and Δ -4, 5-glycuronidase). Residual activity (triplicate) was measured with Z-Phe-Arg-AMC (20 μ M). The relative activity was determined based on the residual protease activity of CatV after incubation (control). Results are expressed as mean \pm SD of three independent experiments. Statistical analyses were performed using Mann-Whitney U test (**: $P < 0.01$; ***: $P < 0.001$; ****: $P < 0.0001$).

activity by Z-Phe-Arg-AMC (Fig. 3D-G).

No endogenous peptidase activity toward Z-Phe-Arg-AMC was detected in the diluted samples prior addition of exogenous CatV. CatV activity was significantly reduced in 1:20 dilution of all MPS types ($P < 0.0001$) and rose progressively along the increasing serial dilutions (Fig. 3D-F). In contrast, no significant difference in the activity of CatV was detectable in non-MPS individuals (Fig. 3G). Pre-treatment of MPS samples with glycosidases (heparinase I, II, and III, chondroitinase B and Δ -4,5-glycuronidase) yielded to a significant retrieval of CatV activity in the presence of MPS-I (Fig. 3D) and MPS-II samples (Fig. 3E). CatV activity was fully recovered in the presence of MPS-III samples (Fig. 3F). Taken together, present results support that accumulation of GAG, including HS, could potentially impair lung CatV activity during MPS.

3.4. Inhibition of cathepsin V by heparan sulfate

Cell-free lysates from wild-type CHO (HS positive strain) and HS-

deficient CHO (HS negative strain) cultures were incubated with recombinant CatV (Fig. 4). A striking difference was observed between HS positive and HS negative CHO samples, since WT lysates but not HS deficient lysates, impaired peptidase CatV activity ($P < 0.0001$) (Fig. 4A). Conversely, CatV activity was fully recovered when HS positive CHO lysates were treated beforehand with heparinases I, II, III, and Δ -4,5-glycuronidase ($P < 0.001$), and thus confirmed that HS is a potent inhibitor of CatV. Moreover, this finding was supported by testing various GAGs at concentrations that mimic those found in liver, lungs and ovaries in MPS models (Chung et al., 2007; Haskins, Otis, Hayden, Jezyk, & Stramm, 1992). Indeed, among GAGs tested, only HS and DS reduced significantly, in a dose dependent manner the peptidase activity of CatV ($P < 0.05$) (Fig. 4B). HS (0.15 %) produced a \sim 5-fold drop of the specificity constant (k_{cat}/K_m), which mostly affected the catalytic activity of CatV (decrease of the k_{cat} value) (Table 2). Increase of the ionic strength by addition of NaCl restored CatV peptidase activity in a dose-dependent manner, suggesting that electrostatic interactions mainly governed binding of CatV to negatively charged HS (Fig. 4C). We

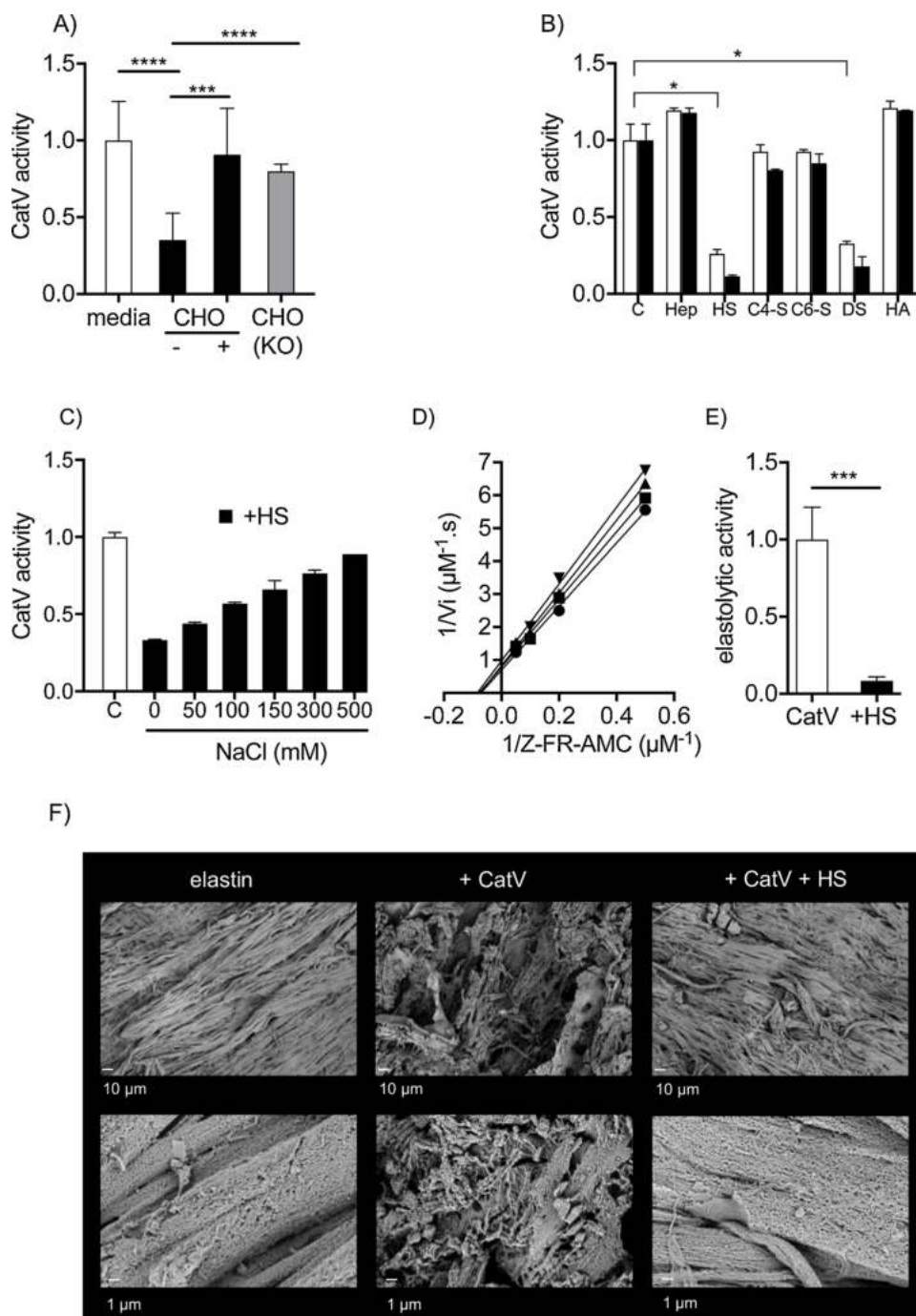


Fig. 4. Inhibition of cathepsin V by heparan sulfate.

A) Recombinant CatV (0.5 nM) was incubated for 10 min in the activity buffer with cell culture media alone (control), CHO cells lysate (-), CHO cell lysate pre-treated with glycosidases (+), and CHO cells lysate lacking HS (KO). B) CatV (0.5 nM) was incubated in the absence (control: C) or in the presence of different GAGs (Hep: low molecular weight heparin; HS: heparan sulfate; C4-S/C6-S: chondroitin 4/6-sulfate; DS: dermatan sulfate; HA: hyaluronic acid) at 0.15 % (weight/volume, w/v) (white bar) and 0.3 % (black bar) in the activity buffer. C) CatV (0.5 nM) activity in the presence of HS (0.1 %) is restored by NaCl. Hydrolysis of Z-Phe-Arg-AMC (20 μ M) was monitored with a spectrofluorometer. The mean values \pm SD of three triplicate independent assays are expressed as relative value for the hydrolysis of Z-Phe-Arg-AMC in each sample (normalized to control = 1). D) Lineweaver-Burk plot analysis of CatV (0.5 nM) velocity (V_i) with varying Z-Phe-Arg-AMC concentrations (1–20 μ M) at a HS concentration of 0–0.01% (0 % : \bullet , 0.001 % : \blacksquare , 0.005 % : \blacktriangle , 0.01 % : \blacktriangledown). E) Elastolytic activity of CatV (1 μ M) in the absence (white bar) or presence of HS (0.15 %, black bar) was measured by the insoluble Congo Red elastin (10 mg/mL) spectrophotometry assay and was expressed as relative value (normalized to control = 1) at 490 nm. F) Representative electron micrographs (SEM) showing the effect of HS (0.3 %) on CatV (1 μ M) elastolytic activity toward bovine neck elastin powder (10 mg/mL) after overnight incubation. Magnification bars, 10 μ m (upper panel) and 1 μ m (lower panel). Results were analyzed using Mann-Whitney U test (P -value *: $P < 0.05$; ***: $P < 0.001$; ****: $P < 0.0001$).

next investigated the mechanism of inhibition of CatV by HS. HS inhibited peptidase CatV activity according to a non-competitive inhibition mechanism (K_i estimated = $11.4 \pm 3 \mu\text{M}$) (Fig. 4D). Then, we incubated CatV with insoluble Congo Red Elastin to determine whether HS could also alter the proteolytic activity of CatV. Fig. 4E revealed that HS (0.15 %) compromised the elastolytic activity of CatV ($90 \pm 2\%$ inhibition, $P < 0.001$). This was further corroborated by SEM analysis. While long elastin fibers (from bovine neck) were broken up into shorter fibrils by CatV, presence of HS impaired fragmentation of elastin fibers (Fig. 4F).

3.5. Binding of heparan sulfate to cathepsin V

CatV (25 kDa) and HS (14 kDa) were eluted at 19.5 mL and at >25

mL, respectively (size exclusion chromatography, Superdex 200 column). Analysis of a mixture of CatV and HS revealed the presence of an additional peak at 200–250 kDa (elution volume: 5–8 mL), which was specifically detected by DMMB assay (Fig. 5A). Also, peptidase CatV activity was detected in both 25 kDa and 200–250 kDa peaks, endorsing that HS bound to CatV in solution. The binding affinity between HS and CatV was calculated by surface plasmon resonance imaging (Fig. 5B). The dissociation equilibrium constant value (K_D) of the HS/CatV complex was $55 \pm 5 \text{ nM}$. This high affinity binding value was in accordance with previous finding above. Molecular modeling studies were further performed to tentatively understand the basis of CatV inhibition and identify putative HS binding sites on CatV (Fig. 5C). According to HS chains vary widely in extent in epimerization and sulfation, we conducted computational experiments using two well-defined HS

Table 2

Kinetic parameters for the hydrolysis of Z-Phe-Arg-AMC by CatV in the presence of GAGs.

GAG (0.15 %)	Sulfatation degree (number of SO ₃ ⁻ by disaccharide)	[Disaccharide] _n	k _{cat} (s ⁻¹)	K _m (μM)	k _{cat} /K _m (×10 ⁶ M ⁻¹ . s ⁻¹)
-	-	-	7.6 ± 0.5	6.9 ± 1.6	11.0 ± 0.9
+ Hep	2.5	L-IdoA2S- α(1→4)-D- GlcNS6S-α(1→4)	5.3 ± 0.3	5.7 ± 1.7	9.0 ± 1.0
+ HS	0.8	D-GlcA-β(1→4)- D-GlcNAc-α(1→4)	1.4 ± 0.2	5.7 ± 1.0	2.4 ± 0.6
+ C4-S	0.9	D-GlcA-β(1→3)- D-GalNAc4S- β(1→4)	5.4 ± 0.2	4.5 ± 0.6	12.0 ± 1.1
+ C6-S	0.9	D-GlcA-β(1→3)- D-GalNAc6S- β(1→4)	8.2 ± 0.9	6.9 ± 1.2	11.8 ± 0.9
+ DS	1.1	L-IdoA-α(1→3)-D- GalNAc4S- β(1→4)	1.3 ± 0.2	4.8 ± 1.2	2.7 ± 0.1

tetrasaccharide models: a highly sulfated variant corresponding to Hep, which has α-L-iduronic acid-2-sulfate-N-sulfo-α-D-glucosamine-6-sulfate (IdoA2S-GlcNS6S) disaccharide units and an unsulfated variant with β-D-glucuronic acid-N-acetyl-α-D-glucosamine (GlcA-GlcNAc) disaccharide unit. Docking scores were obtained for tetrasaccharides as the smallest unit required for specific protein-GAG interactions based on the data available in the PDB (Samsonov & Pisabarro, 2016). Among the 50 top scoring complexes obtained, two major binding sites of unsulfated HS variant were identified on CatV. The most populated cluster (21 poses) was located within the active site cleft (Q19, K20, Q21, G23, S24, C25, N66, G67, and W190) while the second one (15 poses) (V169, G170, Y171, G172, K182, Y183, W184, L185, V186, V200, K201, and I202) located on the backside of the enzyme, away from the catalytic cleft. By contrast, no clusters of Hep were observed in the catalytic domain of CatV (supplementary Fig. 2A). Heparin formed multiple contacts with CatV residues scattered on the backside of the molecule, in the vicinity to the second binding site of unsulfated HS. Furthermore, no binding poses of C4-S tetrasaccharide (β-D-GlcA-N-acetyl-β-D-galactosamine-4-sulfate (GalNAc4S) disaccharide units) were predicted in the active site of CatV (supplementary Fig. 2B), suggesting that unsulfated HS accommodated preferentially the active cleft of the enzyme. These results corroborated the difference in the inhibition of CatV peptidase activity measured by HS, Hep, and C4-S, as previously reported.

3.6. Lys20 is an essential residue within the active-site cleft of cathepsin V for interaction with HS

Human CatV and CatL that share 78 % identity and 85 % homology of protein sequences display similar three-dimensional structures (Fig. 5D). Although both enzymes disclose similar subsite specificities (Choe et al., 2006), high concentration (0.15 %) of cartilage and bone-resident GAGs did not inhibit CatL peptidase activity (Li, Hou, & Brömme, 2000). Docking and MD analysis of unsulfated HS tetrasaccharide on the active site of CatL revealed striking differences with CatV (Fig. 5D). Binding free energy (ΔG_{enz}) calculated by MM-GBSA approach was about twice less favorable for CatL compared to CatV. In addition, electrostatic potential surface of residues bordering the active site of CatL is highly negative, thus less energetically favorable to bind to unsulfated HS ($\Delta G_{enz, el} = 439 \pm 24$ kcal/mol) compared to CatV ($\Delta G_{enz, el} = -54 \pm 18$ kcal/mol).

Next, we analyzed the residues in the CatV cleft that can theoretically interact with unsulfated HS and were different than their counterpart in CatL sequence. The only noticeable difference between CatV and CatL was observed at the position 20 within the active-site cleft. CatV

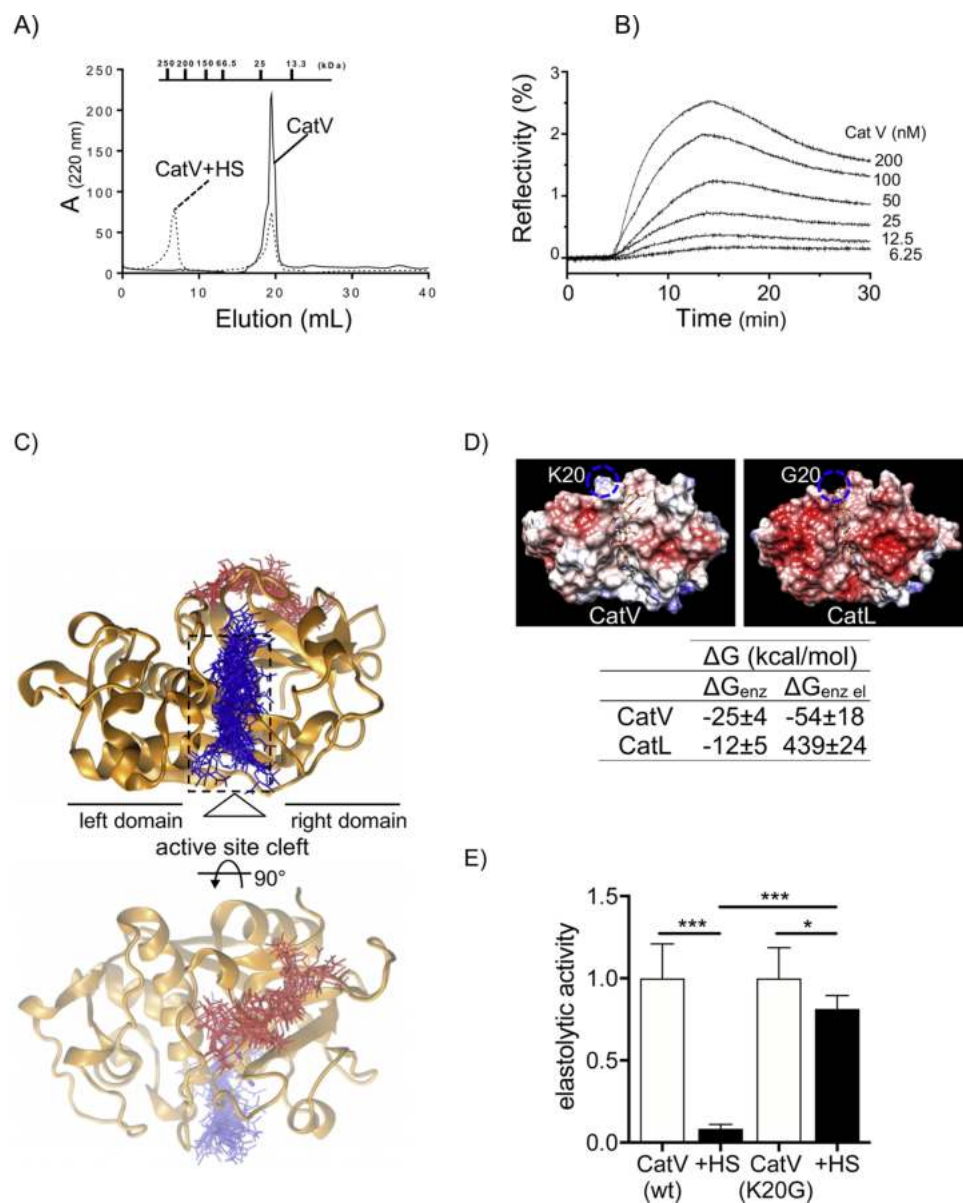
possesses a positively charged lysine residue at position 20, which is replaced by a glycine residue in CatL. Hence, we generated and expressed in *P. pastoris* a K20 G CatV mutant. Specificity constant values for Z-Phe-Arg-AMC hydrolysis by wild-type CatV ($k_{cat}/K_m = 11 \pm 0.9 \times 10^6$ M⁻¹.s⁻¹) and by K20 G CatV mutant ($k_{cat}/K_m = 8.3 \pm 1 \times 10^6$ M⁻¹.s⁻¹) were comparable. This indicates that the overall peptidase activity of the CatV mutant was not affected by this single mutation. Contrary to CatV, addition of HS (0.15 %) did not change significantly the specificity constant of K20 G CatV mutant ($k_{cat}/K_m = 9.63 \pm 1 \times 10^6$ M⁻¹.s⁻¹). Although a slight but significant impairment of the elastolytic activity of K20 G CatV mutant was observed in the presence of HS ($P < 0.05$), K20G CatV still retained a greater elastolytic activity than HS-bound wild-type CatV ($P = 0.0006$) toward Congo Red Elastin (Fig. 4E). This result supported that positively charged Lys20 played a critical role in the binding of HS chain within the active site-cleft of CatV.

3.7. Surfen is a potent antagonist of cathepsin V inhibition by HS and HS-related glycosaminoglycans

In MPS, abnormal levels of heparan sulfate proteoglycans (HSPGs) and accumulation of HS chains (both native or partially degraded forms) are found (De Pasquale & Pavone, 2019; Pan et al., 2005). To address the biological significance of HS attached to a core protein and HS fragments in the inhibition of CatV, the effect of perlecan (a.k.a. heparan sulfate proteoglycan 2) and synthetic HS di- and tetra-saccharides were examined. Perlecan inhibited CatV in a concentration-dependent manner (Fig. 6A), with 80 ± 5% inhibition at a concentration of 2 μg/mL, contrary to aggrecan, a KS/CS-containing proteoglycan (Fig. 6B). To ensure that the observed inhibition was mediated by HS, perlecan was treated with heparinase I. Cleavage of HS chains in perlecan (2 μg/mL) fully restored the peptidase activity of CatV ($P < 0.0001$) (Fig. 6A). Similarly, a consistent decrease in CatV activity was observed with di- and tetrasaccharides of HS (dp2 and dp4, dp: degree of polymerization) (Fig. 6C). Equal percentage (0.001–0.005%, m/v) was used to allow direct comparison between dp2 and dp4. Our results showed that dp4 was significantly more effective than dp2, suggesting that the tetrasaccharide with the repeating unit of N-acetyl-α-D-glucosamine/β-D-glucuronic acid (GlcNAc-GlcA) was the minimal length required to inhibit CatV, which was in agreement with *in silico* studies.

Several HS competitors/antagonists were reported to regulate the expression and/or reduce binding of HS. Of particular interest is Surfen (bis-2-methyl-4-amino-quinolyl-6-carbamide, supplementary Fig. 3A), a chemical compound that binds tightly to HS and was reported to antagonize HS-protein interactions (Schuksz et al., 2008). Therefore, we first investigated the effect of Surfen on the inhibition of CatV *in vitro* by HS and derivatives. We chose concentration of HS, perlecan and dp4 eliciting ~50 % inhibition of CatV activity using Z-Phe-Arg-AMC as a substrate. First, we checked that Surfen, which exhibits weak fluorescence ($\lambda_{ex} = 350$ nm, $\lambda_{em} = 460$ nm) in neutral solution (Schuksz et al., 2008), did not overlap with the fluorescence signal of 7-amido-4-methylcoumarin (AMC) group (supplementary Fig. 3B). Addition of Surfen (10 μM) was sufficient to abolish completely the inhibition of CatV by HS (Fig. 6D), HS-containing proteoglycan perlecan (Fig. 6E), and HS dp4 (Fig. 6F).

We next assessed the effect of Surfen on endogenous cathepsin-mediated elastolytic activity in MPS samples, using Congo Red assays. Interestingly, pretreatment of soluble cell-free supernatants of respiratory secretions with Surfen induced a significant ~6-fold increase of the elastolytic activity compared to untreated MPS samples (MPS-I, II, III specimens) (Fig. 6G). E-64, the broad-spectrum inhibitor of cysteine cathepsins, fully impaired elastolytic activity ($P < 0.0001$), while both odanacatib (ODN), a nitrile-based inhibitor of CatK and CA-074, a selective CatB inhibitor led to a moderate but significant reduction of 23 % and 20 %, respectively. Results endorsed that the elastin degrading activity of MPS samples depends on cysteine cathepsins. Conversely, LHSV, a selective CatS inhibitor, and CatL inhibitor (N-(4-



biphenylacetyl)-S-methylcysteine-(D)-Arg-Phe- β -phenethylamide) did not impair elastinolysis, supporting that the elastolytic activity measured in MPS samples was mainly credited to CatV-related activity.

4. Discussion

Respiratory complications (*i.e.* upper and lower airway obstruction and restrictive pulmonary disease) are typical irreversible features that affect early MPS patients and contribute often with cardiovascular abnormalities to death or disability associated with disease evolution. Current treatments such as hematopoietic stem cell transplantation (HSCT) or enzyme replacement therapy (ERT) are ineffective or insufficiently effective, when they are available (MPS-I, II, IV–A, and VI). Difficulties related to ERT is the need for a weekly highly expensive infusion (~\$130,000/year for a child; twice for an adult). Therefore, there is an imperative need to better understand pathophysiological mechanisms occurring during MPS disease to tentatively prevent its progression. It was reported that an accumulation of ECM components in adeno-tonsillar tissue samples of young MPS patients may contribute to the obstructive phenotype of airway disease (Pal et al., 2018).

Nevertheless, the etiopathogenesis of airway deposits is yet to be elucidated. Few members of the cysteine cathepsin family were examined in the pathophysiology of MPS during the past years (for review: De Pasquale et al., 2020). Abnormal expression of cathepsins B, K, and S were reported in tissues of different MPS animal models (Baldo et al., 2017; Gonzalez et al., 2018; Ohmi et al., 2003; Viana et al., 2020; Wilson et al., 2009). Their dysregulation may alter both ECM remodeling and homeostasis of skeletal, cardiac muscles and heart valves. Also, their overexpression was correlated with growth impairment, joint contractures and cardiovascular disorders found in animal models. As CatV exhibits *in vitro* the highest elastolytic activity yet described among mammalian proteases (Yasuda et al., 2004), we focused on CatV expression and activity in the respiratory secretions of young patients with MPS-I, II and III. CatV was mostly expressed in alveolar macrophages and bronchial epithelial cells of a MPS-I patient. CatV was found both as its proform and its mature form in respiratory specimens (sputum and tracheal aspirates) of MPS patients. However, no significant difference in the expression level of CatV was observed between MPS and non-MPS groups. Also, CatV levels were similar in MPS patients irrespective of a weekly ERT (MPS-I and II) or not (MPS-III). Direction

Fig. 5. Binding of heparan sulfate to cathepsin V.

A) Size-exclusion chromatography profiles of CatV in the absence (solid line) or presence of HS (dashed line). The elution volumes of size standards under identical conditions are shown above the graph. B) CatV-HS binding analyzed by surface plasmon resonance imaging. Compiled sensorgrams of the kinetics of the interactions between CatV (6.25–200 nM) with HS-bearing biochips. C) Clusters from 50 top-scored docking solutions of tetrameric HS (unsulfated) binding to CatV. A "top view" of CatV and "back view" following a 90° rotation around the horizontal axis is shown. The most populated cluster (blue) is located within the active cleft of the enzyme, while the second major cluster (red) is on the backside. D) Docking of tetrameric unsulfated HS within the active site of CatV (PDB:1 FH0) and CatL (PDB:3HHA). MD-based free energy calculations (ΔG) for the obtained binding poses of unsulfated HS were evaluated in the active site (ΔG_{enz}), outside the active site (ΔG_{out}). Electrostatic component of binding energy was reported ($\Delta G_{enz\ el}$) ($\Delta G_{out\ el}$). Surface electrostatic potential of both enzymes is shown. Blue areas correspond to positive charge and red areas to negative charge. Among residues of the active cleft of CatV that are predicted to interact with structural model of HS, K20 was a target residue for mutation to generate a cathepsin *i*-like mutant, K20 G, of CatV. K20 and G20 residues location is depicted by a circle. E) A bar chart analysis showing the effect of HS (0.15 %, black bar) on the elastolytic activity (Congo Red elastin assay) of K20 G CatV mutant compared with wild-type CatV. Results were analyzed using Mann-Whitney *U* test (*P*-value *: *P* < 0.05; ***: *P* < 0.001).

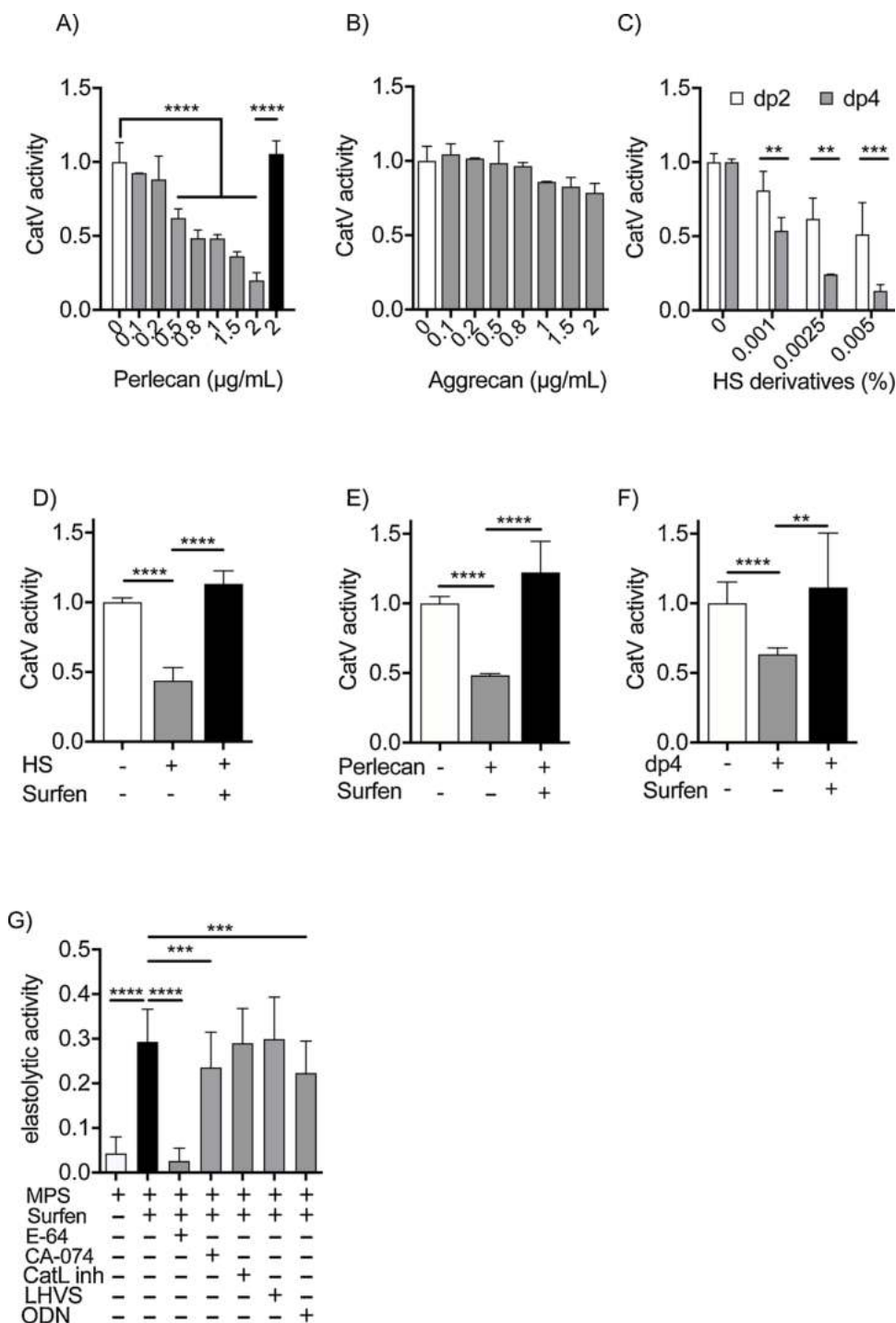


Fig. 6. Inhibition of cathepsin V with HS-like derivatives and influence of Surfen.

A) CatV (0.5 nM) was incubated for 10 min in the activity buffer in the absence (control) or in the presence of increasing concentrations of perlecan (0–2 µg/mL). Assays were also performed with heparinase I-treated perlecan (2 µg/mL, black bar). B) Effect of aggrecan (0–2 µg/mL) and C) synthetic di- and tetrameric heparan sulfate derivative (dp2, dp4; 0.001–0.005%, m/v) on CatV activity. Residual activity was measured with fluorogenic substrate Z-Phe-Arg-AMC (20 µM) and expressed as relative value (normalized to control = 1). D–F) CatV (0.5 nM) was previously incubated in the activity buffer for 10 min with HS from bovine kidney (0.05 %) or perlecan (2000 ng/mL) or dp4 (0.01 %) before adding Surfen (10 µM). Residual activity was measured with the fluorogenic substrate Z-Phe-Arg-AMC (20 µM). G) Surfen enhanced cysteine cathepsins-mediated elastin degradation in cell-free supernatants from MPS-I, II, and III respiratory secretions. Assays were performed with Congo Red elastin (10 mg/mL) incubated overnight under agitation with individual MPS sample (total protein = 30 µg) in the absence and presence of Surfen (10 µM) in the activity buffer at 37 °C. Controls were performed by adding different cathepsin inhibitors : E-64 (100 µM), CA-074 (1 µM), CatL inhibitor (1 µM), LHVS (10 nM) and ODN (1 µM) in the activity buffer at 37 °C. Results were expressed as mean ± SD and were analyzed with Graph-Pad Prism software using Mann-Whitney test, *P*-value **: *P* < 0.01; ***: *P* < 0.001; ****: *P* < 0.0001.

for future research will therefore need to address whether CatV expression is regulated in the course of progressive lung disorders in a larger cohort of untreated patients with MPS. We identified HS as the major sulfated GAG ubiquitously found in MPS-I, II, and III specimen and we established a strong correlation between HS levels and the severity of respiratory-related disorders. Concomitant to our observations, significant correlations were reported between the type of accumulated GAGs, including HS, and the relative involvement of neurological and visceral manifestations in MPS patients (for review: Whitelock & Iozzo, 2005). Thus, high levels of stored HS may be also a useful indicator to predict respiratory disease severity in young patients with MPS. It should be noticed that despite patients with MPS-I and II of

the present cohort underwent ERT treatment, high HS levels were still detected compared with healthy controls. ERT had a negligible impact on pulmonary function in younger children, probably due to limited penetration in the lungs as observed in other organs (Concolino, Deodato, & Parini, 2018). On the other hand, the activity of cathepsins is tightly regulated by linear, negatively charged sulfated Hep, HS, C4-S/C6-S, and DS, unveiling a pattern of repeating disaccharide units, GlcA/IdoA and a hexosamine, GlcNAc/GalNAc (for review: Novinec et al., 2014). The overall activity of cathepsins in MPS specimens was significantly reduced related to *in situ* HS levels, and was negatively correlated with GRSS. Lack of cathepsin-mediated matrix-degrading activity may affect remodeling of lung tissue in MPS, as reported either

in a mouse model of bleomycin-induced lung fibrosis or sarcoidosis (Bühling et al., 2004; Samokhin, Gauthier, Percival, & Brömme, 2011).

Here, we demonstrated that HS-rich MPS sputum and tracheal aspirates inhibited efficiently CatV activity and that HS could form a stable complex with CatV ($K_D = 55 \pm 5$ nM). Moreover, DS that also accumulated in MPS-I and II inhibited CatV *in vitro*, but not C4-S nor C6-S, neither of which contains any IdoA in their disaccharide unit. IdoA is the major uronic acid component of DS and Hep, and in a lesser extent of HS, compared with its epimer β -D-glucuronic acid (GlcA). However, Hep from porcine intestinal mucosal did not hinder the peptidase activity of CatV. It is difficult to explain the ineffectiveness of Hep, with a high level of both sulfation and IdoA, to hinder CatV activity. The low levels of IdoA in the context of domains with a low level sulfation, common to both HS and DS, may explain their CatV inhibitory activity.

Numerous reports suggested a role of HS proteoglycans (HSPGs) in the pathogenesis of MPS (for review: De Pasquale & Pavone, 2019). Here, we used as model the large HSPG perlecan (~500 kDa), which possesses N-terminal ~65 kDa HS side chains (for review: (Gubbiotti, Neill, & Iozzo, 2017)). We demonstrated that the inhibition of CatV by perlecan is mediated by its extended HS chains. Conversely, aggrecan, which mainly possesses CS and KS chains but not HS, did not impair the peptidase activity of CatV, sustaining the critical role of the HS moiety. Moreover, low-molecular-weight GAG fragments have been shown to accumulate in MPS (Fuller, Meikle, & Hopwood, 2004). We identified a synthetic HS-derived tetrasaccharide (dp4) that inhibited potently CatV, suggesting that short oligosaccharides could bind to CatV and impair its activity. These results are in good agreement with molecular modeling, advocating that dp4 binds within the CatV active site while heparin and C4-S are docked in a region distant from the active cleft. Furthermore, it was shown that elastolytic activity of CatV was inhibited *in vitro* by the presence of 0.15 % DS, but also heparin and C4-S/6-S chains (Yasuda et al., 2004). This apparent discrepancy is likely due to the fact that elastin degradation by CatV requires two exosites, which are distant from its active site, and which contribute to elastin binding and its subsequent cleavage (Du et al., 2013). We found that binding sites of heparin and C4-S tetrasaccharides are located on a region nearby to one of the identified elastin-binding exosite (residues Val⁹²-Asn¹⁰⁴) and involved in the elastolytic activity of CatV. It can be speculated that elongation of GAG chains length of heparin and C4-S may hinder the docking of elastin on this CatV exosite, thus suppressing its enzymatic degradation.

Although human cathepsins V and L encompass a close substrate specificity, CatL activity towards peptidyl substrates was unchanged in the presence and the absence of 0.15 % GAGs (Li et al., 2000). Docking studies revealed that among residues involved in HS binding, Lys20 of CatV was of peculiar interest. Analysis of human cysteine cathepsin sequences revealed that a glycine residue is highly conserved in position 20, except for CatW and CatV. Replacement of the positively charged Lys20 by its counterpart in CatL (Gly20) significantly decreased the inhibition of the elastolytic activity by HS, supporting that this basic residue is critical for CatV/HS interactions.

To further address the possibility of an HS antagonist to restore the elastin-degrading activity of CatV in respiratory specimen of patients with MPS, Surfen was chosen based on its ability to block HS-dependent activities (Schuksz et al., 2008). Despite the exact mechanism by which Surfen interacts with HS is unclear, Surfen restored endogenous cathepsin-mediated elastolytic activity in MPS types I, II and III. Using a series of selective inhibitors of human cathepsins, we showed that ~40–45% of the total elastolytic activity against Congo Red elastin can be attributed to both CatB (20 %) and CatK (23 %). Although CatS was reported to degrade substantially elastin in monocyte-derived macrophages (Yasuda et al., 2004), treatment of MPS samples with LHVS did not impair the elastolytic activity. Despite further studies are needed to investigate the role of CatV in MPS pathogenesis, we may assume that CatV mostly contributed to the degradation of elastin, which in turn is impaired by the accumulation of HS in patients with MPS. Accordingly,

selective and safe agents (*i.e.* Surfen and other HS antagonists) (De Pasquale et al., 2018) preventing HS binding to its molecular partners could represent an attractive therapeutic option in MPS patients with lung disorders.

Author contributions

TC and FL designed research; TC, SD, P-MA, KB, SS, DS, and AS performed research; DB, FZ, RJL, FL, and MT contributed new reagents; TC, SD, KB, DS, SS, GL and FL analyzed data; FL wrote the paper. TC, RJL, DB, P-MA, SS, and GL revised the paper. All authors approved the final version of the manuscript.

Competing interests

The authors declare that they have no competing interests.

Acknowledgments

This work received funding from the French association Vaincre les Maladies Lysosomales (VML, Massy, France) and was supported by institutional fundings from the Institut National de la Santé et de la Recherche Médicale (INSERM), the University of Tours and Gago-Sciences (Structure, function and regulation of glycosaminoglycans; GDR 3739, Centre National de la Recherche Scientifique). TC holds a doctoral fellowship from MESRI (Ministère de l'Enseignement Supérieur, de la Recherche et de l'Innovation, France). SD was supported by a French Pediatric Society (SFP) award. KKB holds a BMN (Badania Młodych Naukowców) grant from the Faculty of Chemistry, University of Gdańsk (BMN-538-8370-B249-18) and a grant (UMO-2018/31/N/ST4/01677) from the National Science Centre of Poland (Narodowe Centrum Nauki). SS received funding (grant UMO-2018/30/E/ST4/00037) from the National Science Centre of Poland (Narodowe Centrum Nauki). We are grateful to Dr. Florian Mallèvre and Prof. Thierry Livache (Université Grenoble Alpes, CNRS, SPAM, F-38000 Grenoble, France) for their excellent and skillful assistance in SPRi experiments. Authors acknowledge Prof. Laurent Duca (Université de Reims, Centre National de la Recherche Scientifique (CNRS) 7369, MEDyC, Reims, France) for providing purified bovine neck elastin, Dr. Romain Vivès (Université de Grenoble Alpes, CNRS, Institut de Biologie Structurale, Grenoble, France) for providing the CHO cells, Dr. Michael McDermott (Department of Histopathology, Dublin, Ireland) for providing MPS type I lung tissue samples, and Prof. James McKerrow (Skaggs School of Pharmacy and Pharmaceutical Sciences, University of California, San Diego) for his gift of morpholinourea-leucinyl-homophenylalanine-vinyl-sulfone phenyl inhibitor (LHVS). Authors also acknowledge Dr Julie Chantreuil (Pediatric Intensive Care Unit, University Hospital of Tours, France) for her contribution to sample collection, and patients and their families enrolled in this study.

Appendix A. Supplementary data

Supplementary material related to this article can be found, in the online version, at doi:<https://doi.org/10.1016/j.carbpol.2020.117261>.

References

- Adachi, W., Kawamoto, S., Ohno, I., Nishida, K., Kinoshita, S., Matsubara, K., et al. (1998). Isolation and characterization of human cathepsin V: A major proteinase in corneal Epithelium. *Investigate Ophthalmology and Visual Science*, 39(10), 8.
- Arn, P., Bruce, I. A., Wraith, J. E., Travers, H., & Fallet, S. (2015). Airway-related symptoms and surgeries in patients with mucopolysaccharidosis I. *The Annals of Otolaryngology, and Laryngology*, 124(3), 198–205. <https://doi.org/10.1177/0003489414550154>
- Baldo, G., Tavares, A. M. V., Gonzalez, E., Poletto, E., Mayer, F. Q., Matte, U. da S., et al. (2017). Progressive heart disease in mucopolysaccharidosis type I mice may be mediated by increased cathepsin B activity. *Cardiovascular Pathology*, 27, 45–50. <https://doi.org/10.1016/j.carpath.2017.01.001>

- Barbosa, I., Garcia, S., Barbier-Chassefière, V., Caruelle, J. P., Martelly, I., & Papy-Garcia, D. (2003). Improved and simple micro assay for sulfated glycosaminoglycans quantification in biological extracts and its use in skin and muscle tissue studies. *Glycobiology*, *13*(9), 647–653. <https://doi.org/10.1093/glycob/cwg082>
- Barrett, A. J., Kembhavi, A. A., Brown, M. A., Kirschke, H., Knight, C. G., Tamai, M., et al. (1982). L-trans-Epoxy succinyl-leucylamido(4-guanidino)butane (E-64) and its analogues as inhibitors of cysteine proteinases including cathepsins B, H and L. *The Biochemical Journal*, *201*(1), 189–198. <https://doi.org/10.1042/bj2010189>
- Batzios, S. P., Zafeiriou, D. I., & Papakonstantinou, E. (2013). Extracellular matrix components: an intricate network of possible biomarkers for lysosomal storage disorders? *FEBS Letters*, *587*(8), 1258–1267. <https://doi.org/10.1016/j.febslet.2013.02.035>
- Berger, K. I., Fagundes, S. C., Giugliani, R., Hardy, K. A., Lee, K. S., McArdle, C., et al. (2013). Respiratory and sleep disorders in mucopolysaccharidosis. *Journal of Inherited Metabolic Disease*, *36*(2), 201–210. <https://doi.org/10.1007/s10545-012-9555-1>
- Brömme, D., & Wilson, S. (2011). Role of cysteine cathepsins in extracellular proteolysis. *Extracellular Matrix Degradation*, 23–51. https://doi.org/10.1007/978-3-642-16861-1_2
- Brömme, D., Li, Z., Barnes, M., & Mehler, E. (1999). Human cathepsin V functional expression, tissue distribution, electrostatic surface potential, enzymatic characterization, and chromosomal localization. *Biochemistry*, *38*(8), 2377–2385. <https://doi.org/10.1021/bi982175f>
- Bühling, F., Röcken, C., Brasch, F., Hartig, R., Yasuda, Y., Saftig, P., et al. (2004). Pivotal role of cathepsin K in lung fibrosis. *The American Journal of Pathology*, *164*(6), 2203–2216. [https://doi.org/10.1016/S0002-9440\(10\)63777-7](https://doi.org/10.1016/S0002-9440(10)63777-7)
- Case, D. A., Cerutti, D. S., Cheatham, T. E., III, Darden, T. A., & Duke, R. E. (2017). *Amber 2017*.
- Choe, Y., Leonetti, F., Greenbaum, D. C., Lecaille, F., Bogyo, M., Brömme, D., et al. (2006). Substrate profiling of cysteine proteases using a combinatorial peptide library identifies functionally unique specificities. *The Journal of Biological Chemistry*, *281*(18), 12824–12832. <https://doi.org/10.1074/jbc.M513331200>
- Chowdhury, S. F., Sivaraman, J., Wang, J., Devanathan, G., Lachance, P., Qi, H., et al. (2002). Design of noncovalent inhibitors of human cathepsin L. From the 96-residue proregion to optimized tripeptides. *Journal of Medicinal Chemistry*, *45*(24), 5321–5329. <https://doi.org/10.1021/jm020238t>
- Chung, S., Ma, X., Liu, Y., Lee, D., Tittiger, M., & Ponder, K. P. (2007). Effect of neonatal administration of a retroviral vector expressing α -L-iduronidase upon lysosomal storage in brain and other organs in mucopolysaccharidosis I mice. *Molecular Genetics and Metabolism*, *90*(2), 181–192. <https://doi.org/10.1016/j.ymgme.2006.08.001>
- Concolino, D., Deodato, F., & Parini, R. (2018). Enzyme replacement therapy: Efficacy and limitations. *Italian Journal of Pediatrics*, *44*(S2). <https://doi.org/10.1186/s13052-018-0562-1>. Suppl 2 120.
- De Pasquale, V., & Pavone, L. M. (2019). Heparan sulfate proteoglycans: The sweet side of development turns sour in mucopolysaccharidoses. *Biochimica et Biophysica Acta (BBA) - Molecular Basis of Disease*, *1865*(11), 165539. <https://doi.org/10.1016/j.bbadis.2019.165539>
- De Pasquale, V., Moles, A., & Pavone, L. M. (2020). Cathepsins in the pathophysiology of mucopolysaccharidoses: New perspectives for therapy. *Cells*, *9*(4), 979. <https://doi.org/10.3390/cells9040979>
- De Pasquale, V., Sarogni, P., Pistorio, V., Cerulo, G., Paladino, S., & Pavone, L. M. (2018). Targeting heparan sulfate proteoglycans as a novel therapeutic strategy for mucopolysaccharidoses. *Molecular Therapy - Methods & Clinical Development*, *10*, 8–16. <https://doi.org/10.1016/j.omtm.2018.05.002>
- Du, X., Chen, N. L. H., Wong, A., Craik, C. S., & Brömme, D. (2013). Elastin degradation by cathepsin V requires two exosites. *The Journal of Biological Chemistry*, *288*(48), 34871–34881. <https://doi.org/10.1074/jbc.M113.510008>
- Fuller, M., Meikle, P. J., & Hopwood, J. J. (2004). Glycosaminoglycan degradation fragments in mucopolysaccharidosis I. *Glycobiology*, *14*(5), 443–450. <https://doi.org/10.1093/glycob/cwh049>
- Gonzalez, E. A., Martins, G. R., Tavares, A. M. V., Viegas, M., Poletto, E., Giugliani, R., et al. (2018). Cathepsin B inhibition attenuates cardiovascular pathology in mucopolysaccharidosis I mice. *Life Sciences*, *196*, 102–109. <https://doi.org/10.1016/j.lfs.2018.01.020>
- Gubbiotti, M. A., Neill, T., & Iozzo, R. V. (2017). A current view of perlecan in physiology and pathology: A mosaic of functions. *Matrix Biology*, *57–58*, 285–298. <https://doi.org/10.1016/j.matbio.2016.09.003>
- Gupta, S., O'Meara, A., Wynn, R., & McDermott, M. (2013). Fatal and unanticipated cardiorespiratory disease in a two-year-old child with Hurler syndrome following successful stem cell transplant. *JIMD Reports*, *7*, 119–123. https://doi.org/10.1007/8904_2013_213
- Haskins, M. E., Otis, E. J., Hayden, J. E., Jezyk, P. F., & Stramm, L. (1992). Hepatic storage of glycosaminoglycans in feline and canine models of mucopolysaccharidoses I, VI, and VII. *Veterinary Pathology*, *29*(2), 112–119. <https://doi.org/10.1177/030098589202900203>
- Humphrey, W., Dalke, A., & Schulten, K. (1996). VMD: Visual molecular dynamics. *Journal of Molecular Graphics*, *14*(1), 33–38. [https://doi.org/10.1016/0263-7855\(96\)00018-5](https://doi.org/10.1016/0263-7855(96)00018-5)
- Iozzo, R. V., & Gubbiotti, M. A. (2018). Extracellular matrix: The driving force of mammalian diseases. *Matrix Biology*, *71–72*, 1–9. <https://doi.org/10.1016/j.matbio.2018.03.023>
- Kirschner, K. N., Yongye, A. B., Tschampel, S. M., González-Outeiriño, J., Daniels, C. R., Foley, B. L., et al. (2008). GLYCAM06: A generalizable biomolecular force field. *Carbohydrates. Journal of Computational Chemistry*, *29*(4), 622–655. <https://doi.org/10.1002/jcc.20820>
- Kramer, L., Turk, D., & Turk, B. (2017). The future of cysteine cathepsins in disease management. *Trends in Pharmacological Sciences*, *38*(10), 873–898. <https://doi.org/10.1016/j.tips.2017.06.003>
- Lalmanach, G., Saidi, A., Bigot, P., Chazeirat, T., Lecaille, F., & Wartenberg, M. (2020). Regulation of the proteolytic activity of cysteine cathepsins by oxidants. *International Journal of Molecular Sciences*, *21*(6), 1944. <https://doi.org/10.3390/ijms21061944>
- Lecaille, F., Kaleta, J., & Brömme, D. (2002). Human and parasitic papain-like cysteine proteases: Their role in physiology and pathology and recent developments in inhibitor design. *Chemical Reviews*, *102*(12), 4459–4488. <https://doi.org/10.1021/cr0101656>
- Leighton, S. E. J., Papsin, B., Vellodi, A., Dinwiddie, R., & Lane, R. (2001). Disordered breathing during sleep in patients with mucopolysaccharidoses. *International Journal of Pediatric Otorhinolaryngology*, *58*(2), 127–138. [https://doi.org/10.1016/S0165-5876\(01\)00417-7](https://doi.org/10.1016/S0165-5876(01)00417-7)
- Li, Z., Hou, W.-S., & Brömme, D. (2000). Collagenolytic activity of cathepsin K is specifically modulated by cartilage-resident chondroitin sulfates. *Biochemistry*, *39*(3), 529–536. <https://doi.org/10.1021/bi992251u>
- Liu, R., Xu, Y., Chen, M., Weiwer, M., Zhou, X., Bridges, A. S., et al. (2010). Chemoenzymatic design of heparan sulfate oligosaccharides. *The Journal of Biological Chemistry*, *285*(44), 34240–34249. <https://doi.org/10.1074/jbc.M110.159152>
- Morris, G. M., Goodsell, D. S., Halliday, R. S., Huey, R., Hart, W. E., Belew, R. K., et al. (1998). Automated docking using a Lamarckian genetic algorithm and an empirical binding free energy function. *Journal of Computational Chemistry*, *19*(14), 1639–1662. [https://doi.org/10.1002/\(SICI\)1096-987X\(19981115\)19:14<1639::AID-JCC10>3.0.CO;2-B](https://doi.org/10.1002/(SICI)1096-987X(19981115)19:14<1639::AID-JCC10>3.0.CO;2-B)
- Muenzer, J. (2011). Overview of the mucopolysaccharidoses. *Rheumatology*, *50*(suppl 5), v4–v12. <https://doi.org/10.1093/rheumatology/ker394>
- Muhlebach, M. S., Wooten, W., & Muenzer, J. (2011). Respiratory manifestations in mucopolysaccharidoses. *Paediatric Respiratory Reviews*, *12*(2), 133–138. <https://doi.org/10.1016/j.prrv.2010.10.005>
- Naudin, C., Joulin-Giet, A., Couetdic, G., Plésiat, P., Szymanska, A., Gorna, E., et al. (2011). Human cysteine cathepsins are not reliable markers of infection by *Pseudomonas aeruginosa* in cystic fibrosis. *PLoS One*, *6*, e25577. <https://doi.org/10.1371/journal.pone.0025577>
- Naumnik, W., Ossolińska, M., Płońska, I., Chyczewska, E., & Nikliński, J. (2014). Endostatin and cathepsin-V in bronchoalveolar lavage fluid of patients with pulmonary sarcoidosis. *Lung Cancer and Autoimmune Disorders*, 55–61. https://doi.org/10.1007/5584_2014_26
- Novinec, M., Lenarčič, B., & Turk, B. (2014). Cysteine cathepsin activity regulation by glycosaminoglycans. *BioMed Research International*, *2014*, 1–9. <https://doi.org/10.1155/2014/309718>
- Ohmi, K., Greenberg, D. S., Rajavel, K. S., Ryazantsev, S., Li, H. H., & Neufeld, E. F. (2003). Activated microglia in cortex of mouse models of mucopolysaccharidoses I and IIIB. *Proceedings of the National Academy of Sciences*, *100*(4), 1902–1907. <https://doi.org/10.1073/pnas.252784899>
- Onufriev, A., Case, D. A., & Bashford, D. (2002). Effective born radii in the generalized Born approximation: The importance of being perfect. *Journal of Computational Chemistry*, *23*(14), 1297–1304. <https://doi.org/10.1002/jcc.10126>
- Pal, A. R., Mercer, J., Jones, S. A., Bruce, I. A., & Bigger, B. W. (2018). Substrate accumulation and extracellular matrix remodelling promote persistent upper airway disease in mucopolysaccharidosis patients on enzyme replacement therapy. *PLoS One*, *13*(9), e0203216. <https://doi.org/10.1371/journal.pone.0203216>
- Pan, C., Nelson, M. S., Reyes, M., Koodie, L., Brazil, J. J., Stephenson, E. J., et al. (2005). Functional abnormalities of heparan sulfate in mucopolysaccharidosis-I are associated with defective biologic activity of FGF-2 on human multipotent progenitor cells. *Blood*, *106*(6), 1956–1964. <https://doi.org/10.1182/blood-2005-02-0657>
- Panitz, N., Theisgen, S., Samsonov, S. A., Gehrcke, J.-P., Baumann, L., Bellmann-Sickert, K., et al. (2016). The structural investigation of glycosaminoglycan binding to CXCL12 displays distinct interaction sites. *Glycobiology*, *26*(11), 1209–1221. <https://doi.org/10.1093/glycob/cwv059>
- Pichert, A., Samsonov, S. A., Theisgen, S., Thomas, L., Baumann, L., Schiller, J., et al. (2012). Characterization of the interaction of interleukin-8 with hyaluronan, chondroitin sulfate, dermatan sulfate and their sulfated derivatives by spectroscopy and molecular modeling. *Glycobiology*, *22*(1), 134–145. <https://doi.org/10.1093/glycob/cwr120>
- Reiser, J., Adair, B., & Reinheckel, T. (2010). Specialized roles for cysteine cathepsins in health and disease. *The Journal of Clinical Investigation*, *120*(10), 3421–3431. <https://doi.org/10.1172/JCI42918>
- Rutten, M., Ciet, P., van den Biggelaar, R., Oussoren, E., Langendonk, J. G., van der Ploeg, A. T., et al. (2016). Severe tracheal and bronchial collapse in adults with type II mucopolysaccharidosis. *Orphanet Journal of Rare Diseases*, *11*(1), 50. <https://doi.org/10.1186/s13023-016-0425-z>
- Sage, J., Malleuvre, F., Barbarin-Costes, F., Samsonov, S. A., Gehrcke, J.-P., Pisabarro, M. T., et al. (2013). Binding of chondroitin 4-sulfate to cathepsin S regulates its enzymatic activity. *Biochemistry*, *52*(37), 6487–6498. <https://doi.org/10.1021/bi400925g>
- Samokhin, A. O., Gauthier, J. Y., Percival, M. D., & Brömme, D. (2011). Lack of cathepsin activities alter or prevent the development of lung granulomas in a mouse model of sarcoidosis. *Respiratory Research*, *12*(1), 13. <https://doi.org/10.1186/1465-9921-12-13>
- Samsonov, S. A., & Pisabarro, M. T. (2016). Computational analysis of interactions in structurally available protein–glycosaminoglycan complexes. *Glycobiology*, *8*, 850–861.

- Santamaría, I., Velasco, G., Cazorla, M., Fueyo, A., Campo, E., & Lã, C. (1998). Cathepsin L2, a novel human cysteine proteinase produced by breast and colorectal carcinomas. *Cancer Research*, 8, 1624–1630.
- Schuksz, M., Fuster, M. M., Brown, J. R., Crawford, B. E., Ditto, D. P., Lawrence, R., et al. (2008). Surfen, a small molecule antagonist of heparan sulfate. *Proceedings of the National Academy of Sciences*, 105(35), 13075–13080. <https://doi.org/10.1073/pnas.0805862105>
- Spira, D., Stypmann, J., Tobin, D. J., Petermann, I., Mayer, C., Hagemann, S., et al. (2007). Cell type-specific functions of the lysosomal protease cathepsin L in the heart. *The Journal of Biological Chemistry*, 282(51), 37045–37052. <https://doi.org/10.1074/jbc.M703447200>
- Stapleton, M., Arunkumar, N., Kubaski, F., Mason, R. W., Tadao, O., & Tomatsu, S. (2018). Clinical presentation and diagnosis of mucopolysaccharidoses. *Molecular Genetics and Metabolism*, 125(1–2), 4–17. <https://doi.org/10.1016/j.ymgme.2018.01.003>
- Tolosa, E., Li, W., Yasuda, Y., Wienhold, W., Denzin, L. K., Lautwein, A., et al. (2003). Cathepsin V is involved in the degradation of invariant chain in human thymus and is overexpressed in myasthenia gravis. *The Journal of Clinical Investigation*, 112(4), 517–526. <https://doi.org/10.1172/JCI200318028>
- Viana, G. M., Priestman, D. A., Platt, F. M., Khan, S., Tomatsu, S., & Pshzhetsky, A. V. (2020). Brain pathology in mucopolysaccharidoses (MPS) patients with neurological forms. *Journal of Clinical Medicine*, 9(2), 396. <https://doi.org/10.3390/jcm9020396>
- Vidak, E., Javoršek, U., Vizovišek, M., & Turk, B. (2019). Cysteine cathepsins and their extracellular roles: Shaping the microenvironment. *Cells*, 8(3), 264. <https://doi.org/10.3390/cells8030264>
- Vizovišek, M., Fonović, M., & Turk, B. (2019). Cysteine cathepsins in extracellular matrix remodeling: Extracellular matrix degradation and beyond. *Matrix Biology*, 75–76, 141–159. <https://doi.org/10.1016/j.matbio.2018.01.024>
- Vizovišek, M., Vidak, E., Javoršek, U., Mikhaylov, G., Bratovš, A., & Turk, B. (2020). Cysteine cathepsins as therapeutic targets in inflammatory diseases. *Expert Opinion on Therapeutic Targets*, 24(6), 573–588. <https://doi.org/10.1080/14728222.2020.1746765>
- Whitelock, J. M., & Iozzo, R. V. (2005). Heparan sulfate: A complex polymer charged with biological activity. *Chemical Reviews*, 105(7), 2745–2764. <https://doi.org/10.1021/cr010213m>
- Wilson, S., Hashamiyan, S., Clarke, L., Saftig, P., Mort, J., Dejica, V. M., et al. (2009). Glycosaminoglycan-mediated loss of cathepsin K collagenolytic activity in MPS I contributes to osteoclast and growth plate abnormalities. *The American Journal of Pathology*, 175(5), 2053–2062. <https://doi.org/10.2353/ajpath.2009.090211>
- Yasuda, Y., Li, Z., Greenbaum, D., Bogyo, M., Weber, E., & Brömme, D. (2004). Cathepsin V, a novel and potent elastolytic activity expressed in activated macrophages. *The Journal of Biological Chemistry*, 279(35), 36761–36770. <https://doi.org/10.1074/jbc.M403986200>